ORNL-2537
Reactors-General cy. 4

AN INVESTIGATION OF THE STRESSES IN A DISCONTINUITY REGION OF A PRESSURE VESSEL

B. L. Greenstreet

OAK RIDGE NATIONAL LABORATORY ATOMIC ENERGY COMMISSION U.S.

OAK RIDGE NATIONAL LABORATORY
operated by
UNION CARBIDE CORPORATION
for the
U.S. ATOMIC ENERGY COMMISSION

Printed in USA. Price $2.00 cents. Available from the
Office of Technical Services
U. S. Department of Commerce
Washington 25, D. C.

ORNL-2537

Contract No. W-7405-eng-26

Reactor Projects Division

AN INVESTIGATION OF THE STRESSES IN A DISCONTINUITY REGION OF A PRESSURE VESSEL

B. L. Greenstreet

Submitted as a thesis to the Graduate Council of The University of Tennessee in partial fulfillment of the requirements for the degree of Master of Science

DATE ISSUED

JUL 8 1958

OAK RIDGE NATIONAL LABORATORY
Oak Ridge, Tennessee
operated by
UNION CARBIDE CORPORATION
for the
U.S. ATOMIC ENERGY COMMISSION

SUMMARY

A thin-walled cylindrical pressure vessel was held at 1500°F in an inert atmosphere until creep rupture occurred. The vessel was made of Inconel, and it had a flat-plate head at one end. This configuration yielded high discontinuity stresses in the region of the head to shell junction.

As the vessel deformed due to creep of the material, its configuration changed. In order to determine the effect of this continual change in configuration upon the stress distribution at the flat-plate head end of the shell, the test was interrupted at various time intervals. The specimen was removed from the furnace, and it was loaded by internal pressure at room temperature. The resulting strains were measured using strain gages, and the corresponding stresses were calculated. In addition to the strain measurements, the dimensions of the vessel were also obtained.

Initially, the maximum axial stress in the cylinder which existed where the flat head and cylinder were joined was approximately ten times the circumferential membrane stress. However, the high stresses at the junction of the head and cylinder decreased with creep time, and the vessel failed in a region where the membrane stresses predominated throughout the test. The circumferential strain in this region was approximately twelve percent while it was approximately four percent in the high stress region.

TABLE OF CONTENTS

PAGE

INTRODUCTION 1

TEST APPARATUS AND PROCEDURE 3

RESULTS 7

DISCUSSION AND CONCLUSIONS 11

BIBLIOGRAPHY 55

LIST OF TABLES

TABLE		PAGE
I.	Axial Location of Each Station on Cylinder	14
II.	Theoretical Stresses for Cylinder	15
III.	Theoretical Stresses for Flat Head	17
IV.	Initial Strain Measurements	18
V.	Strain Measurements After 30 Hours of Creep	19
VI.	Strain Measurements After 500 Hours of Creep	20
VII.	Strain Measurements After 1000 Hours of Creep	21
VIII.	Strain Measurements After 3472 Hours of Creep	22
IX.	Initial Dimensionless Stresses	23
X.	Dimensionless Stresses After 30 Hours of Creep	24
XI.	Dimensionless Stresses After 500 Hours of Creep	25
XII.	Dimensionless Stresses After 1000 Hours of Creep	26
XIII.	Dimensionless Stresses After 3472 Hours of Creep	27
XIV.	Averaged Dimensionless Stresses	28
XV.	Distance of Each Axial Station from Center of Outside Surface of Head as a Function of Creep Time	29
XVI.	Outside Diameter of Cylinder at Each Axial Station as a Function of Creep Time	30
XVII.	Change in Outside Diameter of Cylinder at Each Axial Station and Deformation at the Center of the Head as a Function of Creep Time	31

LIST OF TABLES (continued)

TABLE		PAGE
XVIII.	Outside Diameter of Ruptured Vessel at Designated Angular Orientations and at Various Distances From Center of Outside Surface of Head	32
XIX.	Measured Profile Outside Surface of Head of Ruptured Vessel	33

LIST OF FIGURES

FIGURE		PAGE
1.	Photograph of Cylinder and Flat Head Unit	34
2.	Pressure Vessel Assembly After 500 Hours of Creep	35
3.	Locations of Reference Lines and Designated Stations on Vessel	36
4.	Pressure Vessel Assembly With Strain Gages in Place	37
5.	Total Axial Stress at Outside Surface of Cylinder Vs Distance Along Axis	38
6.	Total Tangential Stress at Outside Surface of Cylinder Vs Distance Along Axis	39
7.	Total Radial Stress at Outside Surface of Head Vs Radius	40
8.	Total Tangential Stress at Outside Surface of Head Vs Radius	41
9.	Total Stress at Outside Surface of Cylinder Vs Creep Time - Station 1	42
10.	Total Stresses at Outside Surface of Cylinder Vs Creep Time - Station 3	43
11.	Total Stresses at Outside Surface of Cylinder Vs Creep Time - Station 5	44
12.	Total Stresses at Outside Surface of Head Vs Creep Time	45

LIST OF FIGURES (continued)

FIGURE		PAGE
13.	Change in Outside Diameter of Cylinder Vs Distance Along Axis	46
14.	Change in Outside Diameter of Cylinder Vs Creep Time - Station 1	47
15.	Change in Outside Diameter of Cylinder Vs Creep Time - Stations 1' and 2	48
16.	Change in Outside Diameter of Cylinder Vs Creep Time - Stations 3, 4 and 5	49
17.	Deformation of Center of Head Vs Creep Time	50
18.	Pressure Vessel at End of 1000 Hours of Creep	51
19.	Pressure Vessel at End of 3472 Hours of Creep	52
20.	Photograph of Vessel Showing Region of Failure	53

INTRODUCTION

In thin-walled pressure vessels, localized stresses occur due to a change in radius or slope of the meridian. The meridian is a line that represents the intersection of the mid surface of the vessel walls and a plane containing the axis of the vessel. This change in radius or slope produces a change in direction of the stress resultant; hence, bending is induced. Local bending is also induced by an abrupt change in wall thickness. One of the more important cases of a change in radius or slope of the meridian arises where a head joins the body of a vessel. The additional stresses set up are called "discontinuity stresses", and the region in which they occur is called the "discontinuity region".

When designing a pressure vessel, the engineer must assess the importance of discontinuity stresses in regard to their effect upon its structural integrity. At temperatures where creep of the material is negligible, no adverse effects are encountered if the stresses in a discontinuity region are greater than the yield strength of the material but less than its ultimate strength (1)[1]. This is true if the vessel is not subjected to cyclic loadings which produce fatigue. However, for vessels operating at temperatures that allow creep of the material, creep rupture may occur prematurely in the discontinuity region, or, on the other hand, the growth and distortion in this region may render the vessel unusable even though rupture has not occurred.

---

[1]Numbers in parentheses refer to similarly numbered references in bibliography at end of paper.

Consider a vessel operating under conditions that make creep an important factor. The growth and distortion can be expected to yield a marked stress redistribution. The possibility of a redistribution creates a need for information concerning the role of discontinuity stresses in producing distortion or failure of the vessel. This information would allow more precise determination of the wall thickness for a given container, and, consequently, more effective use of material. The need is brought into focus in applications wherein there is internal heat generation or constant heat flux through the vessel walls. The resultant thermal stresses, coupled with the pressure stresses, often lead to a compromise in the overall design.

This paper describes an experimental investigation of the stresses and deformations in a thin-walled pressure vessel operated at a temperature which allowed the material to creep. The primary purpose of the investigation was to study stress-time histories in a discontinuity region of the vessel, and to determine the role of the discontinuity stresses in establishing the creep-rupture lifetime of that vessel. In addition to the stress-time histories, deformation-time histories were also obtained.

TEST APPARATUS AND PROCEDURE

The specimen used in this study was a cylindrical vessel made of Inconel with a flat-plate head at one end. The outside diameter of the cylindrical portion was 1.69 in., and its thickness was 0.040 in. The cylinder was effectively infinite in length, and the head was 0.080 in. thick. Since the purpose of the study was to investigate the stresses and deformations in the region where the flat head and cylinder were joined, the cylinder and head were made as an integral unit which was machined from bar stock to avoid a weld joint at their junction (see Fig 1). This unit was welded to an ellipsoidal head into which had been mounted a tube for pressurizing the vessel. A thermocouple well passed through the center of the ellipsoidal head to provide a means for measuring the temperature inside the assembly. The complete pressure vessel assembly can be seen in Fig 2.

In order to locate the points where strain and dimensional measurements were to be made, lines were scribed on the outside surface of the vessel. Two diametral lines at 90° to each other, along with an 0.50 in. radius circle whose center was at the intersection of these lines, were made on the surface of the head. Six axial stations along the cylinder were established by peripheral lines.

The axial stations of the cylinder were designated as 1, 1', 2, 3, 4, and 5 with station number one being nearest the end of the shell. The four stations at the intersection of the diametral lines and the 0.50 in. radius circle on the head were designated as number six, and the center of the head was station seven (see Fig 3).

In plotting both the stress and deformation data, the edge of the cylinder was assumed to be at a distance equal to the head thickness (0.080 in.) away from the edge of the vessel. Using this location as the origin, the distance of each station along the axis of the undeformed cylinder is given in Table I.

It was not possible to make strain measurements at the temperatures required to produce creep in Inconel. Instead, the vessel was allowed to creep under a pressure loading and at a specified temperature for a known length of time. Then it was subjected to a uniform, internal pressure at room temperature, and the resulting strains were measured using 1/16 in., SR-4 type, strain gages. The data thus obtained provided a means for determining the effect of the creep deformation upon the magnitudes of the stresses and strains resulting from a given pressure loading.

Radial and tangential strains in the case of the head and axial and circumferential (or tangential) strains in the cylinder were measured for two pressure levels. Two levels were used so that the linearity of the gages could be checked. The initial measurements were taken at internal pressures of 80 and 200 psi while pressures of 100 and 200 psi were used for the remaining ones. Figure 4 shows the vessel with strain gages in place.

In all but a few cases, two gages were used to measure the strain in a given direction at each station. However, as the creep deformation of the cylinder progressed, it became increasingly more difficult to mount a strain gage in the proper location at station one. Therefore, by increasing the number of gages used at this station, a means was provided for obtaining more accurate average strain values.

The strains were measured prior to beginning the test. Following this the specimen was sealed in a container which was then filled with an inert gas. The container was placed in a furnace and the specimen was held at a temperature of 1500°F while subjected to an internal pressure of 75 psi. It was maintained at these conditions for a specified length of time; at the end of this period, the specimen was removed from the furnace and container, and strain measurements were again made. This sequence was repeated until strain data after 3472 hours of creep were obtained. Finally, the specimen was held at 1500°F and 275 psi internal pressure until rupture of the material occurred. The total creep time was 3517 hours, and the rupture took place along an axial line near station five.

The internal pressure corresponding to each set of strain data was measured by the use of an Ashcroft, Bourdon type gage. This gage was calibrated using an Amthor, dead weight tester.

The dimensions of the vessel were also obtained at room temperature. Diameter measurements were taken at each station along the cylinder. The deformation at the center of the head was measured with reference to the outside edge. The initial diameter measurements were made through the use of a micrometer while subsequent measurements were made using a shadowgraph comparator. The final measurements, which were taken after rupture of the specimen had occurred, included complete deformation versus radius dimensions of the head.

The initial diameter measurements were taken for two angular orientations, 90° apart. However, due to the presence of the pressurizing tube, thermocouple wells, and the flange (see Fig 4), subsequent measurements which were taken by using the comparator could be made for only one angular orientation of the vessel. At the end of the testing program, the vessel was cut apart at the weld joint between the cylinder and the ellipsoidal head. This made it possible to obtain dimensions of the shell at any angular orientation.

RESULTS

The total theoretical stress distributions in both the cylinder and flat head were calculated for the purpose of comparing the analytical and experimental results. They are tabulated for unit pressure in Tables II and III, and they are plotted in Figs 5 through 8. The theoretical distributions were obtained using the method outlined by Timoshenko[1].

In addition to the initial strain measurements which were taken for pressure loadings at room temperature, similar strain data were obtained after the vessel had been allowed to creep for periods of 30, 50, 1000 and 3472 hours. The stresses were calculated from the strain data using Hooke's law for a biaxial stress system (5). The modulus of elasticity, E, was taken as 30×10^6 psi, and Poisson's ratio, μ, was 0.30.

The strains at the outside surface of the vessel are given in Tables IV through VIII for the designated stations and directions. In this study, the main interest, as far as the stress histories in the cylinder were concerned, centered around the maximum stresses in the discontinuity region and the stresses in a region that was not influenced by the discontinuity forces. Therefore, strain measurements were not taken at all of the stations each time a set of data was obtained.

---

[1]See pp. 406 through 410 of (2). The equations for describing the cylinder are given on p. 393 of this reference. Those for the head are given on pp. 62 through 64 of (2) and pp. 237 and 238 of (3). The specific method of calculating the stresses in a cylindrical vessel with a flat head is given in (4).

Thus, a vacancy in the tables indicates the absence of a gage. The dashed lines in Table IV indicate that the gage was not working.

At each station, the average of the strain measurements for a given direction and pressure level was calculated, and these data were used to determine the stresses. The resulting dimensionless stress values[2] are tabulated in Tables IX through XIII.

The dimensionless stresses associated with the two pressure levels were, in turn, averaged to give representative values for each station. These average stresses are given in Table XIV. They are plotted with creep time as a parameter in Figs 5 through 8[3]. Figures 9 through 12 give the average dimensionless stresses as a function of time for various stations.

The creep deformation at the center of the flat head and the diameters of the cylinder corresponding to each axial station were measured after creep times of 30, 100, 200, 1000 and 3472 hours. The diameters of the cylinder at each axial station are given in Table XVI. The changes in cylinder diameter and the deformation at the center of the head are listed in Table XVII. The change in diameter of the cylinder as a function of axial distance with creep time as a parameter is

---

[2]Dimensionless stresses are given throughout this report. These were obtained by dividing the stresses by the corresponding pressure levels.

[3]The distance along the axis in these figures refers to that of the undeformed specimen. The measured distance of each axial station from the center of the outside surface of the head as a function of creep time is given in Table XV.

shown in Fig 13. These diameter changes and the deformation of the center of the head are plotted as a function of creep time in Figs 14, 15, 16 and 17.

The diameter measurements for the cylinder and the deformation versus radius measurements for the head which were obtained after rupture had occurred are given in Tables XVIII and XIX. The diameters of the cylinder were measured in the plane passing through both the vessel centerline and the axial crack and in two planes which were at angles of 60 and 120 degrees to the first. The crack was taken as the zero degree reference and, looking along the axis of the cylinder from the flat-head end, the angles were measured in a clockwise direction. Since the head was very nearly a true spherical segment, the only deformation versus radius measurements recorded were those for the plane through the crack.

The head deformed into a quasi-spherical shape. At the end of 1000 hours of creep, the spherical radius of the central portion of the head was approximately 2 in. This radius had decreased to approximately 1.62 in. at the end of 3472 hours, and it was 1.406 in. when rupture occurred.

The cylinder also deformed into a quasi-spherical shape. However, a reverse in meridional curvature occurred near station one. For times corresponding to those at which the radius at the center of the head was measured, the minimum radius in the vicinity of station one was 0.19, 0.11, and 0.041 in., respectively.

The specimen after 500 hours of creep is shown in Fig 2. It is also shown after 1000 hours in Fig 18 and after 3472 hours in Fig 19. A photograph that was taken of the vessel after creep rupture had occurred is shown in Fig 20. The axial crack which marked the vessel's failure can be seen. Small axial cracks were also visible on the opposite side of the vessel near the same axial location, and a crack had developed at the inside surface along the head to shell juncture.

DISCUSSION AND CONCLUSIONS

The functions giving the stresses in the cylinder, when plotted, have a damped, wave form. The length of these waves is given by (see p. 166 of (3)),

$$\ell = 2\pi \sqrt[4]{\frac{a^2h^2}{3(1-\mu^2)}}$$

where

a = radius

h = thickness

μ = Poisson's ratio.

The wave length for the specimen tested was 0.89 in. This short wave length was accompanied by a very large stress gradient in the discontinuity region. Hence, the axial location of each gage in this region had undue effect upon the strain measurements obtained. Also, the size of the gages (1/16 in.) was large compared with the wave length. These factors contributed the largest uncertainties in the reported data.

The modulus of elasticity and Poisson's ratio were assumed to be invariant throughout the lifetime of the vessel. The validity of this assumption bears investigation. However, the stress-time histories given here are actually direct portrayals of the strain-time histories.

As can be seen from Figs 5, 6, 7 and 8, the magnitudes and distributions of the calculated stresses and those obtained from strain measurements are in reasonable agreement. However, it must be remembered when comparing the magnitudes of the theoretical and experimental stresses that any difference in physical dimensions or in elastic constants from those used would enter into this comparison.

The stresses in the head as calculated from the strain data decreased continuously with time. However, so long as the deformation at the center of the head was less than half the thickness, the stresses were very close to those for the flat head (see Figs 7 and 8).

The stresses at station one of the cylinder also decreased with time. However, the rate of deformation at this point, as measured by a change in diameter, did not follow the high, initial rate of decrease in axial stress.

The diameter measurements taken at the axial stations of the cylinder after 30 hours of creep were less than those obtained prior to subjecting the vessel to creep conditions. This general decrease in diameter was probably due to the influence of the discontinuity force and moment. However, when the specimen was subjected to creep conditions for longer periods of time, the cylinder increased in diameter at stations 3, 4 and 5. Rupture occurred in the cylinder near the point of maximum diameter increase.

In the region of failure, the circumferential strain was approximately twelve per cent. On the other hand, the maximum circumferential strain in the discontinuity region was approximately four per cent.

Two important conclusions stand out from this test. These are:

1) Failure occurred in a region where the pressure forces, as opposed to the discontinuity forces, predominated.

2) The maximum circumferential strain did not occur in the discontinuity region.

Since Inconel is a very ductile material, caution should be used in applying the above results to vessels of other materials. A specimen made of a material with less ductility than Inconel might experience failure in the discontinuity region. This conjecture is made because the axial strain near the head to shell junction reached a large value before rupture occurred.

It is recommended that more tests similar to the one reported here be made using vessels of various materials. In this connection, it would be desirable to use a specimen whose stresses have a long wave length compared with the strain gage dimensions. Also, the overall size of the vessel should be chosen to facilitate the installation of strain gages. The consequence of not giving proper consideration to this last item is well depicted in Fig 4.

TABLE I

AXIAL LOCATION OF EACH STATION ON CYLINDER

Station	Distance From Edge of Vessel (in.)	Distance From Edge of Cylinder (in.)
1	0.111	0.031
1'	0.143	0.063
2	0.260	0.180
3	0.380	0.300
4	0.580	0.500
5	1.080	1.000

TABLE II

THEORETICAL STRESSES FOR CYLINDER

Axial Distance (in.)	Inside Surface[a] σ_x/p	Inside Surface[a] σ_θ/p	Outside Surface σ_x/p	Outside Surface σ_θ/p
0.000	172.7	38.8	-152.1	-58.6
0.028	131.6	18.0	-111.0	-54.8
0.057	96.1	4.2	-75.4	-47.3
0.085	66.7	-4.0	-46.1	-37.8
0.113	43.3	-7.9	-22.7	-27.6
0.141	25.4	-8.6	-4.8	-17.7
0.170	12.5	-7.2	8.1	-8.5
0.198	3.7	-4.4	17.0	-0.4
0.226	-1.8	-0.9	22.4	6.4
0.254	-4.7	2.9	25.3	11.9
0.283	-5.6	6.5	26.3	16.1
0.367	-2.1	15.4	22.7	22.9
0.452	3.8	20.1	16.8	24.0
0.537	8.2	21.8	12.4	23.0
0.622	10.3	21.8	10.3	21.8

[a] σ_x/p = Dimensionless axial stress

σ_θ/p = Dimensionless circumferential (or tangential) stress.

TABLE II (continued)

THEORETICAL STRESSES FOR CYLINDER

Axial Distance (in.)	Inside Surface[a]		Outside Surface	
	σ_x/p	σ_θ/p	σ_x/p	σ_θ/p
0.707	11.0	21.3	9.6	20.9
0.791	10.9	20.9	9.7	20.6
0.876	10.7	20.7	10.0	20.5
0.961	10.4	20.6	10.2	20.5
1.017	10.4	20.6	10.3	20.5

TABLE III

THEORETICAL STRESSES FOR FLAT HEAD

Radius (in.)	Inside Surface[b] σ_r/p	σ_t/p	Outside Surface σ_r/p	σ_t/p
0.00	-70.8	-70.8	81.1	81.1
0.10	-68.8	-69.7	79.1	79.9
0.20	-63.0	-66.3	73.3	76.6
0.30	-53.3	-60.7	63.6	71.0
0.40	-39.8	-53.0	50.1	63.2
0.50	-22.4	-42.9	32.7	53.2
0.60	-1.1	-30.7	11.4	40.9
0.70	24.0	-16.2	-13.7	26.5
0.80	53.0	0.5	-42.7	9.8
0.825	60.8	5.1	-50.9	5.1

[b] σ_r/p = Dimensionless radial stress

σ_t/p = Dimensionless tangential stress.

TABLE IV

INITIAL STRAIN MEASUREMENTS

Station	Direction	Strains in in./in. x10^6 Pressure = 80 psi		Pressure = 200 psi	
1	Axial	-202	-159	-493	-374
1	Tangential	-37	-32	-92	-80
2	Axial	55	18	126	68
2	Tangential	-5	--	-14	--
3	Axial	37	38	82	109
3	Tangential	32	28	71	69
4	Axial	14	14	46	34
4	Tangential	41	36	93	91
5	Axial	0	6	41	27
5	Tangential	37	32	96	86
6	Radial	37	28	101	95
6	Tangential	105	94	261	255
7		129		349	

TABLE V

STRAIN MEASUREMENTS AFTER 30 HRS. OF CREEP

Station	Direction	Strains in in./in. x10^6 Pressure = 100 psi		Pressure = 200 psi	
1	Axial	-177	-163	-354	-326
1	Tangential	-53	-53	-107	-109
2	Axial				
2	Tangential				
3	Axial	45		86	
3	Tangential	25	27	52	54
4	Axial				
4	Tangential				
5	Axial	11	14	20	23
5	Tangential	38		74	
6	Radial	38	54	79	104
6	Tangential	109	97	213	197
7		160		323	

TABLE VI

STRAIN MEASUREMENTS AFTER 500 HRS. OF CREEP

Station	Direction	Strains in in./in. x10^{6} Pressure = 100 psi		Pressure = 200 psi	
1	Axial	-118	-128	-233	-258
1	Tangential	-40	-40	-85	-80
2	Axial	42	42	77	82
2	Tangential	-10	-5	-20	-10
3	Axial	42	47	77	87
3	Tangential	27	32	52	62
4	Axial				
4	Tangential				
5	Axial	10	7	20	12
5	Tangential	37		72	
6	Radial	42	47	82	97
6	Tangential	42	40	87	85
7		80		150	

TABLE VII

STRAIN MEASUREMENTS AFTER 1000 HRS. OF CREEP

		Strains in in./in. x10^6			
Station	Direction	Pressure = 100 psi		Pressure = 200 psi	
1	Axial	-63	-68	-127	-127
		-76		-152	
1	Tangential	-21	-25	-42	-51
		-30	-17	-59	-34
2	Axial	30	34	55	68
2	Tangential	4	2	9	3
3	Axial	25	25	51	51
3	Tangential	21	17	47	34
4	Axial	8		17	
4	Tangential	34		63	
5	Axial	8	4	17	8
5	Tangential	34	30	68	59
6	Radial	47	47	85	89
6	Tangential	21	21	47	42
7		42		85	

TABLE VIII

STRAIN MEASUREMENTS AFTER 3472 HRS. OF CREEP

Station	Direction	Strains in in./in. x10^6 Pressure = 100 psi		Pressure = 200 psi	
1	Axial	-42	-34	-88	-67
1	Tangential	-17	-8	-34	-17
		-19		-36	
2	Axial	25	25	50	55
2	Tangential	8	13	13	25
3	Axial	14	21	27	38
3	Tangential	25	25	50	46
4	Axial	10	6	23	14
4	Tangential	38	34	76	67
5	Axial	10	4	23	13
5	Tangential	38	34	71	67
6	Radial	25	25	59	55
6	Tangential	17	13	29	25
7		25		46	

TABLE IX

INITIAL DIMENSIONLESS STRESSES

Station	Direction	Pressure = 80 psi	Pressure = 200 psi
1	Axial	-81.3	-78.3
1	Tangential	-37.7	-36.8
2	Axial	22.8	15.9
2	Tangential	5.1	2.6
3	Axial	19.6	19.9
3	Tangential	17.4	16.8
4	Axial	10.7	11.5
4	Tangential	18.2	17.7
5	Axial	5.8	10.5
5	Tangential	15.0	17.3
6	Radial	26.4	29.9
6	Tangential	46.6	49.0
7		71.3	77.3

TABLE X

DIMENSIONLESS STRESSES AFTER 30 HRS. OF CREEP

Station	Direction	Pressure = 100 psi	Pressure = 200 psi
1	Axial	-63.2	-63.2
1	Tangential	-35.3	-35.7
2	Axial		
2	Tangential		
3	Axial	18.0	17.4
3	Tangential	13.3	13.3
4	Axial		
4	Tangential		
5	Axial	8.1	7.4
5	Tangential	14.3	13.6
6	Radial	26.2	26.0
6	Tangential	39.7	39.6
7		71.0	71.6

TABLE XI

DIMENSIONLESS STRESSES AFTER 500 HRS. OF CREEP

Station	Direction	Pressure = 100 psi	Pressure = 200 psi
1	Axial	-46.0	-46.2
1	Tangential	-26.3	-26.8
2	Axial	13.6	13.0
2	Tangential	1.7	1.5
3	Axial	18.4	16.9
3	Tangential	15.0	14.0
4	Axial		
4	Tangential		
5	Axial	6.8	6.5
5	Tangential	13.6	13.1
6	Radial	19.4	19.7
6	Tangential	18.8	19.8
7		35.5	33.3

TABLE XII

DIMENSIONLESS STRESSES AFTER 1000 HRS. OF CREEP

Station	Direction	Pressure = 100 psi	Pressure = 200 psi
1	Axial	-25.9	-25.4
1	Tangential	-15.0	-14.8
2	Axial	11.3	13.6
2	Tangential	4.4	4.3
3	Axial	10.6	10.7
3	Tangential	9.2	9.6
4	Axial	6.1	6.1
4	Tangential	12.3	11.6
5	Axial	5.5	5.5
5	Tangential	11.6	11.6
6	Radial	18.1	17.2
6	Tangential	11.9	12.1
7		18.8	18.9

TABLE XIII

DIMENSIONLESS STRESSES AFTER 3472 HRS. OF CREEP

Station	Direction	Pressure = 100 psi	Pressure = 200 psi
1	Axial	-14.4	-14.7
1	Tangential	-8.9	-8.9
2	Axial	9.7	9.9
2	Tangential	6.2	5.9
3	Axial	8.6	8.0
3	Tangential	10.4	9.9
4	Axial	6.4	6.8
4	Tangential	13.0	13.1
5	Axial	6.1	6.6
5	Tangential	12.9	12.7
6	Radial	10.1	11.1
6	Tangential	7.6	7.6
7		11.2	10.2

TABLE XIV

AVERAGED DIMENSIONLESS STRESSES

Station	Direction	Initial	30 Hrs.	500 Hrs.	1000 Hrs.	3472 Hrs.
1	Axial	-79.8	-63.2	-46.1	-25.4	-14.6
1	Tangential	-37.3	-35.5	-26.5	-14.8	-8.9
2	Axial	19.4	--	13.3	12.5	9.8
2	Tangential	3.9	--	1.6	4.4	6.1
3	Axial	19.8	17.7	17.7	10.7	8.3
3	Tangential	17.1	13.3	14.5	9.4	10.2
4	Axial	11.1	--	--	6.1	6.6
4	Tangential	18.0	--	--	11.9	13.1
5	Axial	10.5	7.8	6.7	5.5	6.4
5	Tangential	16.2	14.0	13.4	11.6	12.8
6	Radial	28.2	26.1	19.6	17.7	10.6
6	Tangential	47.8	39.7	19.3	12.0	7.6
7		74.3	71.3	35.4	18.9	10.7

TABLE XV

DISTANCE OF EACH AXIAL STATION FROM CENTER OF OUTSIDE SURFACE OF HEAD AS A FUNCTION OF CREEP TIME

	Dimensions in in. Creep Time - Hrs.					
Station	30	100	200	500	1000	3472
1	0.131	0.145	0.168	0.207	0.245	0.312
1'	0.166	--	0.202	0.239	0.277	0.342
2	0.283	0.296	0.318	0.356	0.395	0.460
3	0.403	0.414	0.438	0.477	0.516	0.581
4	0.602	0.616	0.638	0.676	0.716	0.782
5	1.102	1.114	1.139	1.176	1.216	1.384

TABLE XVI

OUTSIDE DIAMETER OF CYLINDER AT EACH AXIAL STATION
AS A FUNCTION OF CREEP TIME

	Diameters in in. Creep Time - Hrs.					
Station	0(ave.)	30	100	200	1000	3472
1	1.6903	1.6871	1.6854	1.6822	1.6648	1.6421
1'	1.6903	1.6873	1.6865	1.6845	1.6701	1.6549
2	1.6905	1.6887	1.6892	1.6895	1.6880	1.6995
3	1.6900	1.6892	1.6913	1.6930	1.6968	1.7263
4	1.6904	1.6891	1.6915	1.6939	1.6988	1.7442
5	1.6904	1.6880	1.6922	1.6935	1.6984	1.7507

TABLE XVII

CHANGE IN OUTSIDE DIAMETER OF CYLINDER AT EACH AXIAL STATION AND DEFORMATION[c] AT THE CENTER OF THE HEAD AS A FUNCTION OF CREEP TIME

Station	Dimensions in in. Creep Time - Hrs. 30	100	200	1000	3472
1	-0.0032	-0.0049	-0.0081	-0.0255	-0.0450
1'	-0.0030	-0.0038	-0.0059	-0.0202	-0.0354
2	-0.0032	-0.0013	-0.0010	-0.0025	+0.0090
3	-0.0018	+0.0013	+0.0030	+0.0067	+0.0363
4	-0.0013	+0.0011	+0.0035	+0.0084	+0.0538
5	-0.0032	+0.0009	+0.0022	+0.0071	+0.0603
7(Center of head)	+0.019	+0.031	+0.055	+0.139	+0.207

[c]This deformation was measured with respect to the edge of the head.

TABLE XVIII

OUTSIDE DIAMETER OF RUPTURED VESSEL AT DESIGNATED ANGULAR ORIENTATIONS AND AT VARIOUS DISTANCES FROM CENTER OF OUTSIDE SURFACE OF HEAD

Dimensions in in.				
		Angular Orientation		
Identification	Distance	0°	60°	120°
Outside Corner of Head	0.265	1.648	1.648	1.650
Min. Dia. of Cylinder	0.323	1.605	1.604	1.607
Station 1	0.363	1.631	1.634	1.636
Station 1'	0.392	1.656	1.656	1.662
Station 2	0.504	1.734	1.733	1.737
Station 3	0.631	1.784	1.785	1.780
Station 4	0.830	1.842	1.841	1.831
Station 5	1.332	1.885	1.913	1.895

TABLE XIX

MEASURED PROFILE OUTSIDE SURFACE OF
HEAD OF RUPTURED VESSEL

Dimensions in in.	
Radius	Deformation[d]
0.0	0.265
0.196	0.253
0.392	0.213
0.588	0.137
0.784	0.029
0.824	0.0

[d]This deformation was measured with respect to the edge of the head as before.

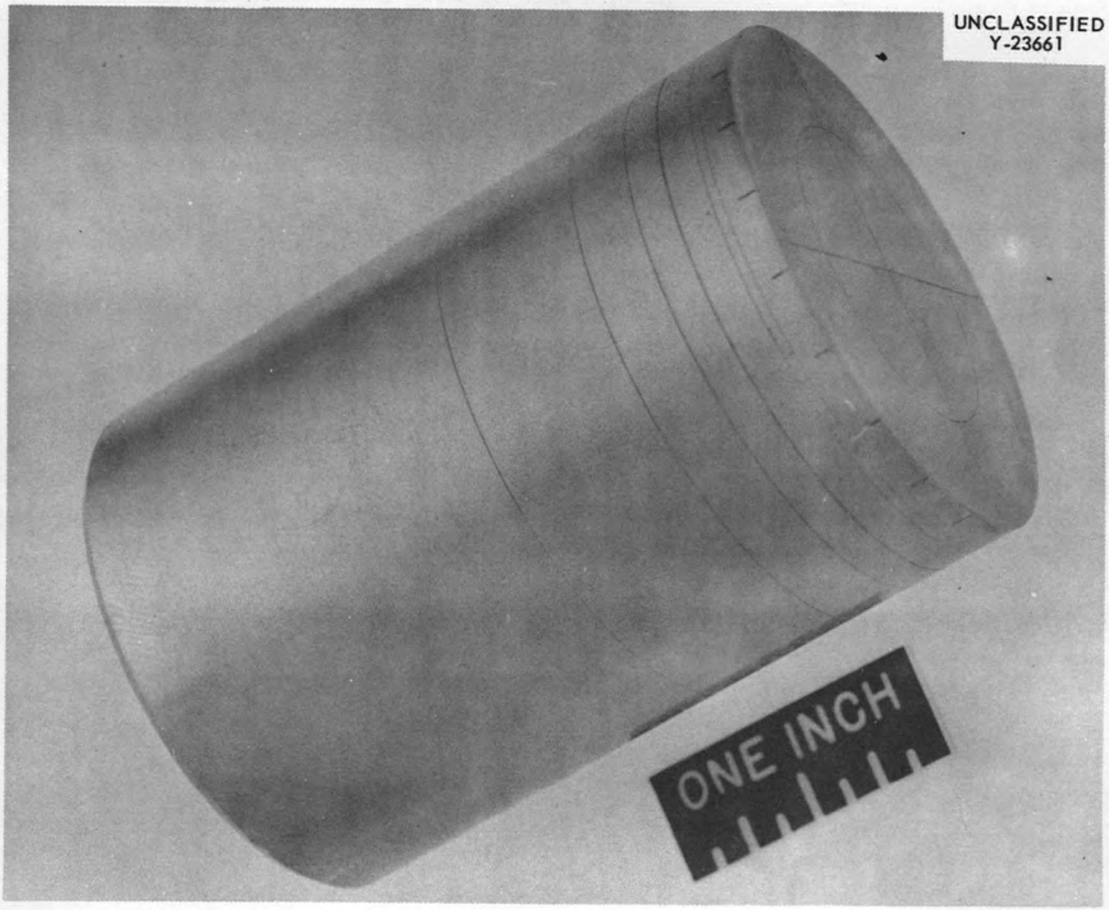

FIGURE 1. PHOTOGRAPH OF CYLINDER AND FLAT HEAD UNIT

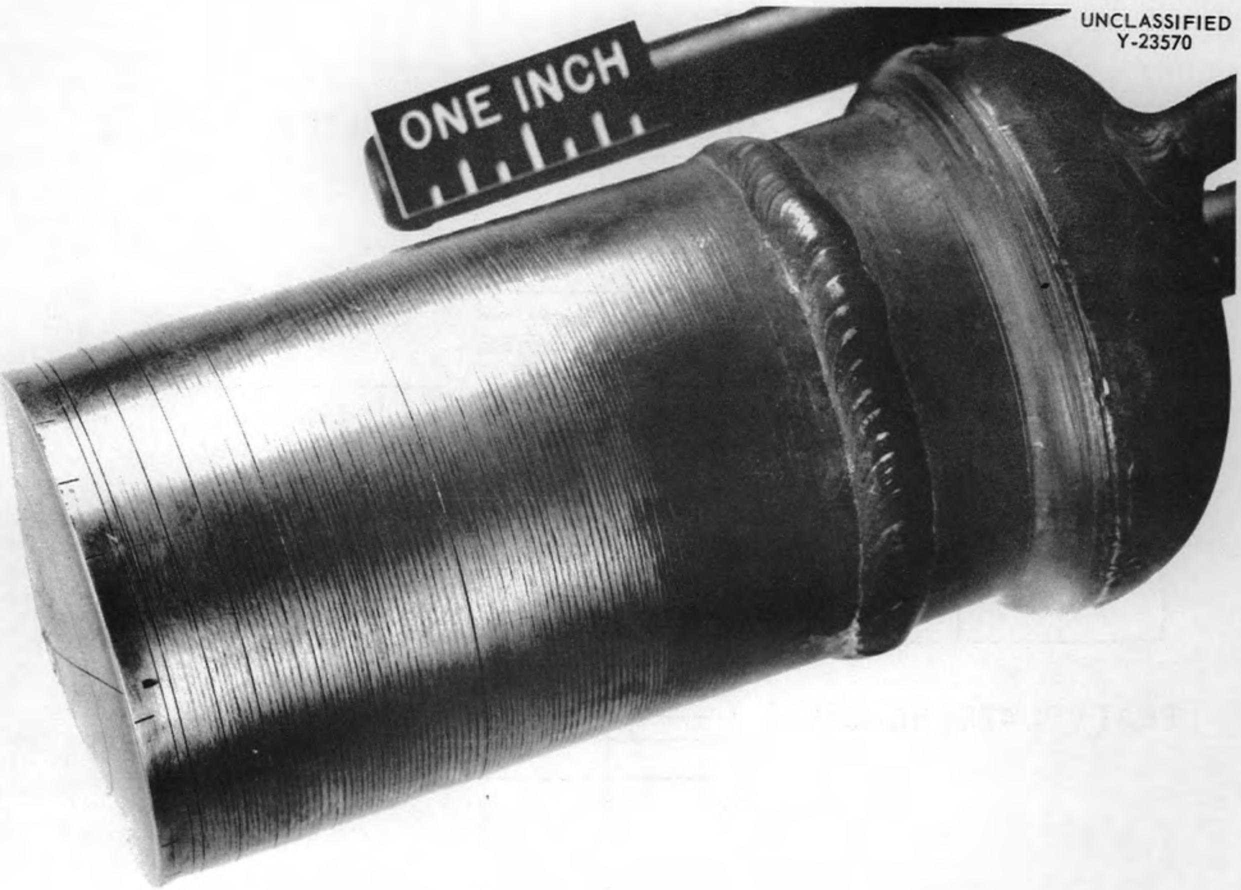

FIGURE 2. PRESSURE VESSEL ASSEMBLY AFTER 500 HRS. OF CREEP

UNCLASSIFIED
ORNL-LR-DWG. 30485

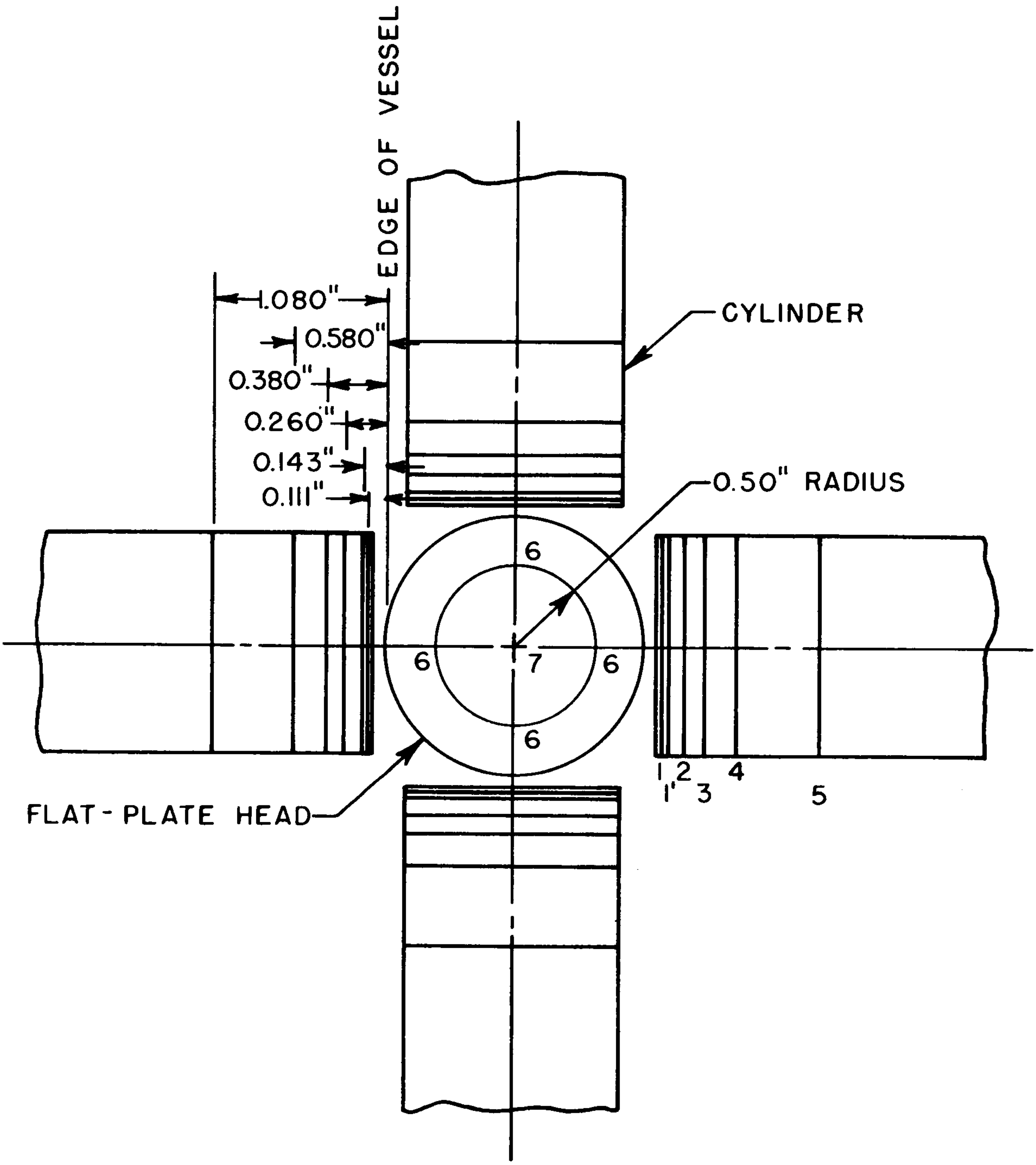

FIGURE 3. LOCATIONS OF REFERENCE LINES AND DESIGNATED STATIONS ON VESSEL.

UNCLASSIFIED
UNIVERSITY OF TENNESSEE

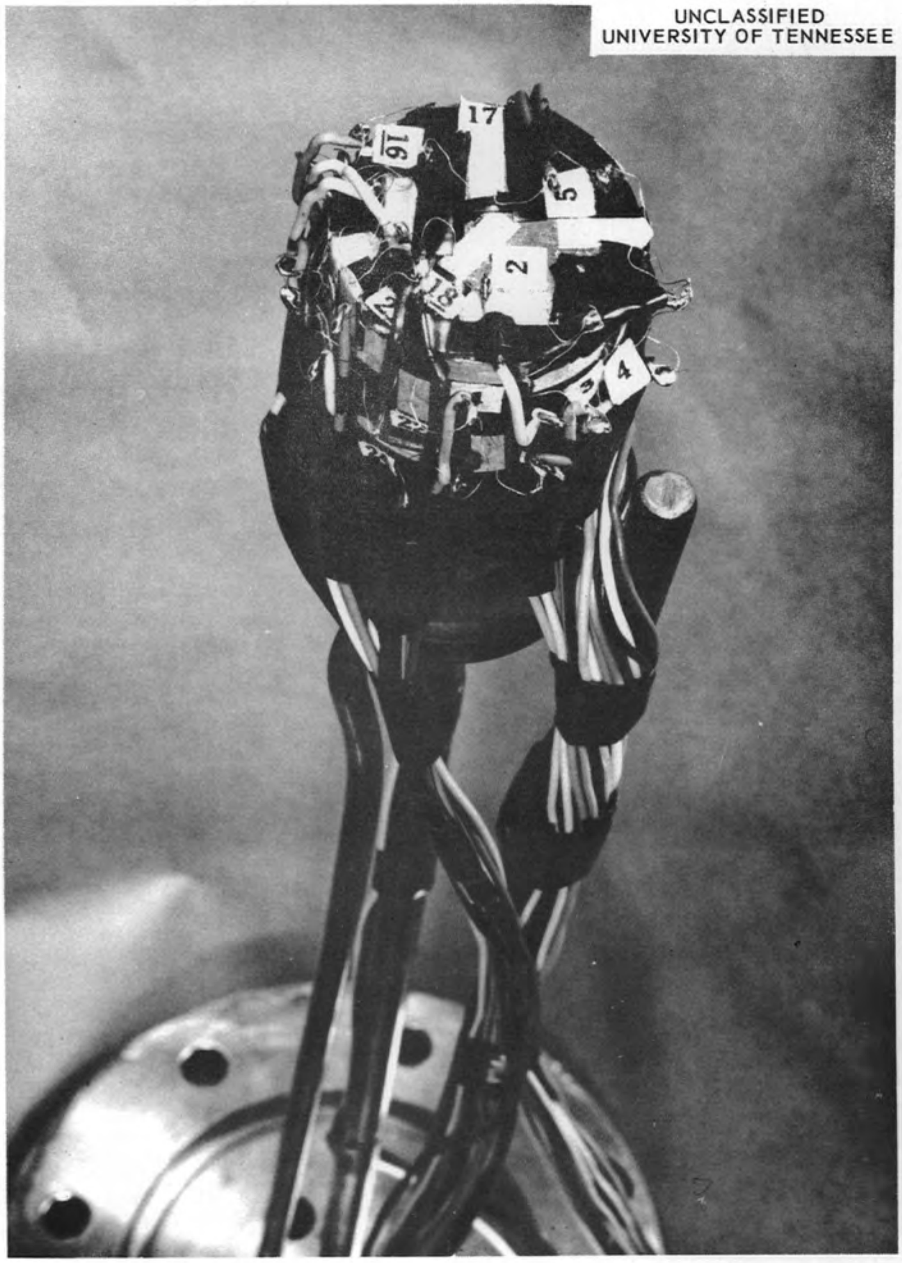

FIGURE 4. PRESSURE VESSEL ASSEMBLY WITH STRAIN GAGES IN PLACE

UNCLASSIFIED
ORNL-LR-DWG. 30486

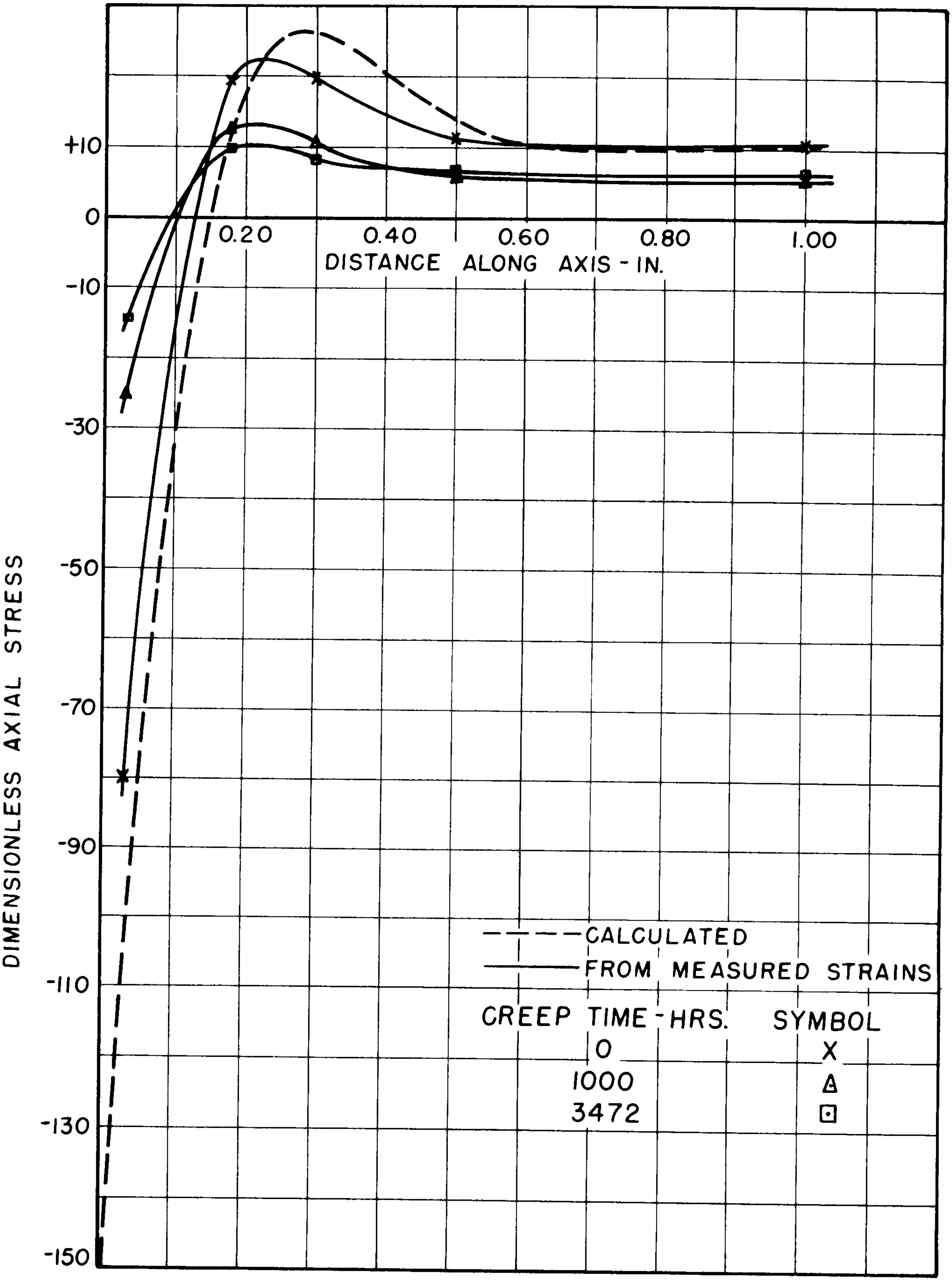

FIGURE 5. TOTAL AXIAL STRESS AT OUTSIDE SURFACE OF CYLINDER VS. DISTANCE ALONG AXIS

UNCLASSIFIED
ORNL-LR-DWG. 30487

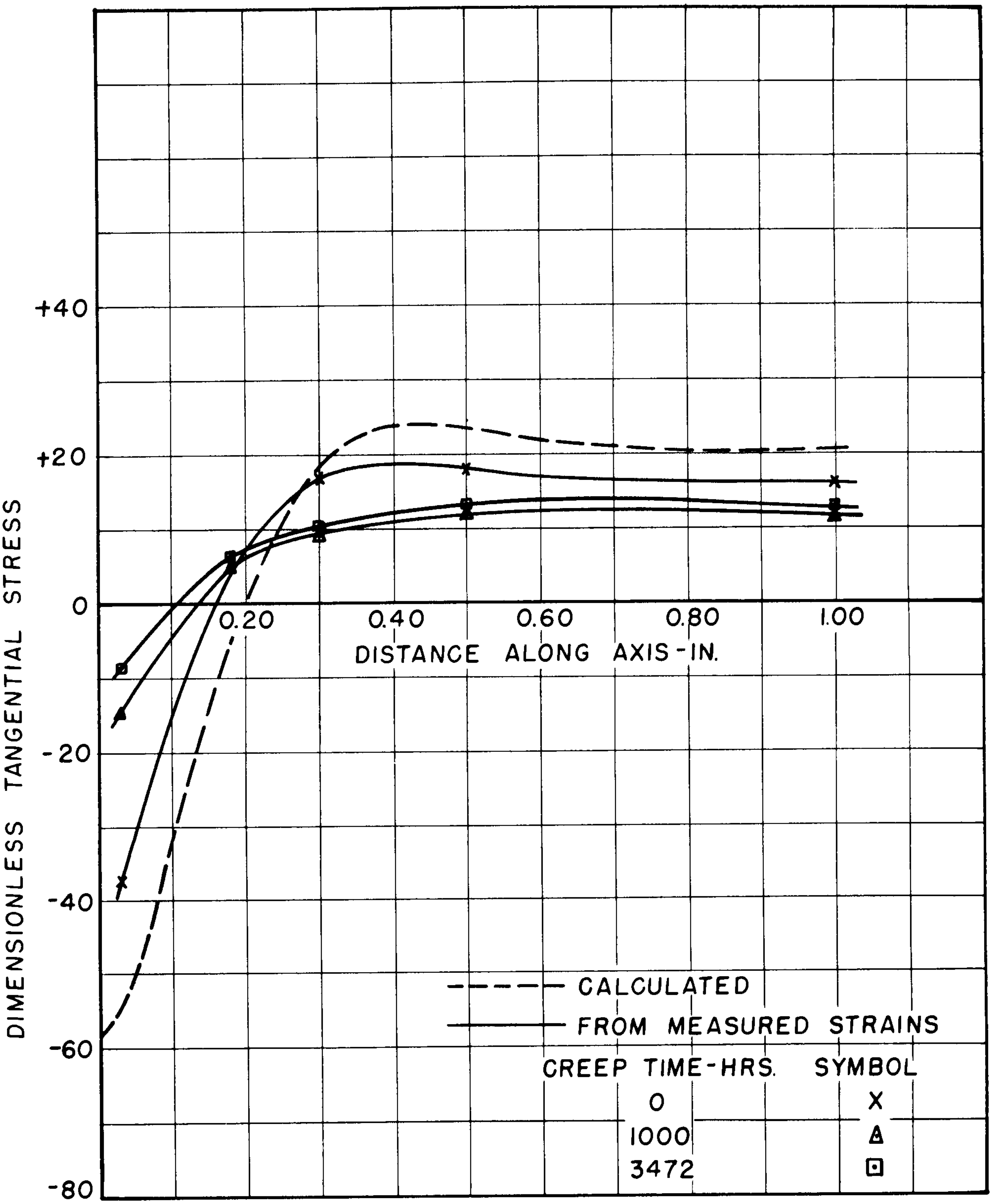

FIGURE 6. TOTAL TANGENTIAL STRESS AT OUTSIDE SURFACE OF CYLINDER VS. DISTANCE ALONG AXIS

UNCLASSIFIED
ORNL-LR-DWG. 30488

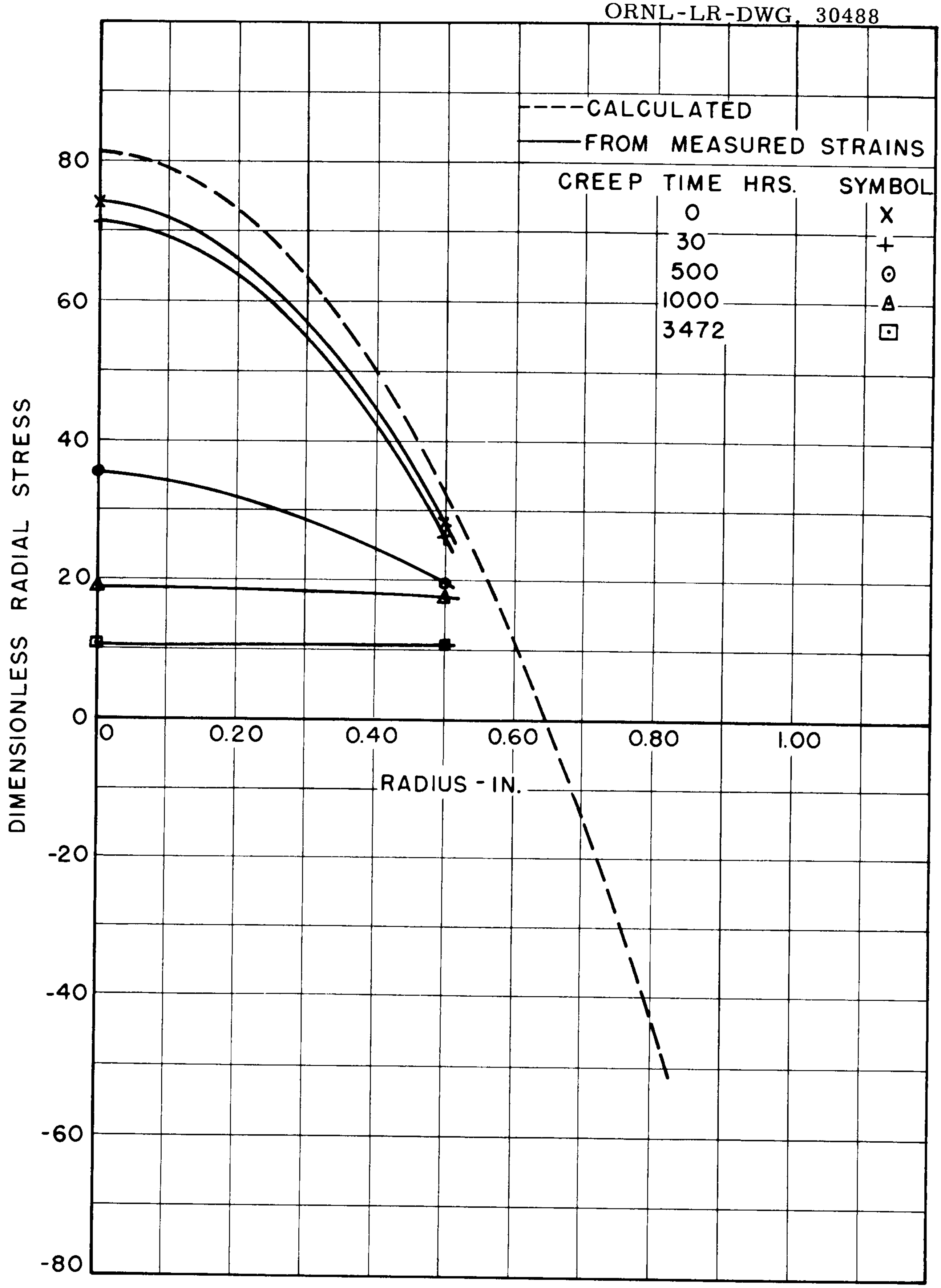

FIGURE 7. TOTAL RADIAL STRESS AT OUTSIDE SURFACE OF HEAD VS. RADIUS

UNCLASSIFIED
ORNL-LR-DWG. 30489

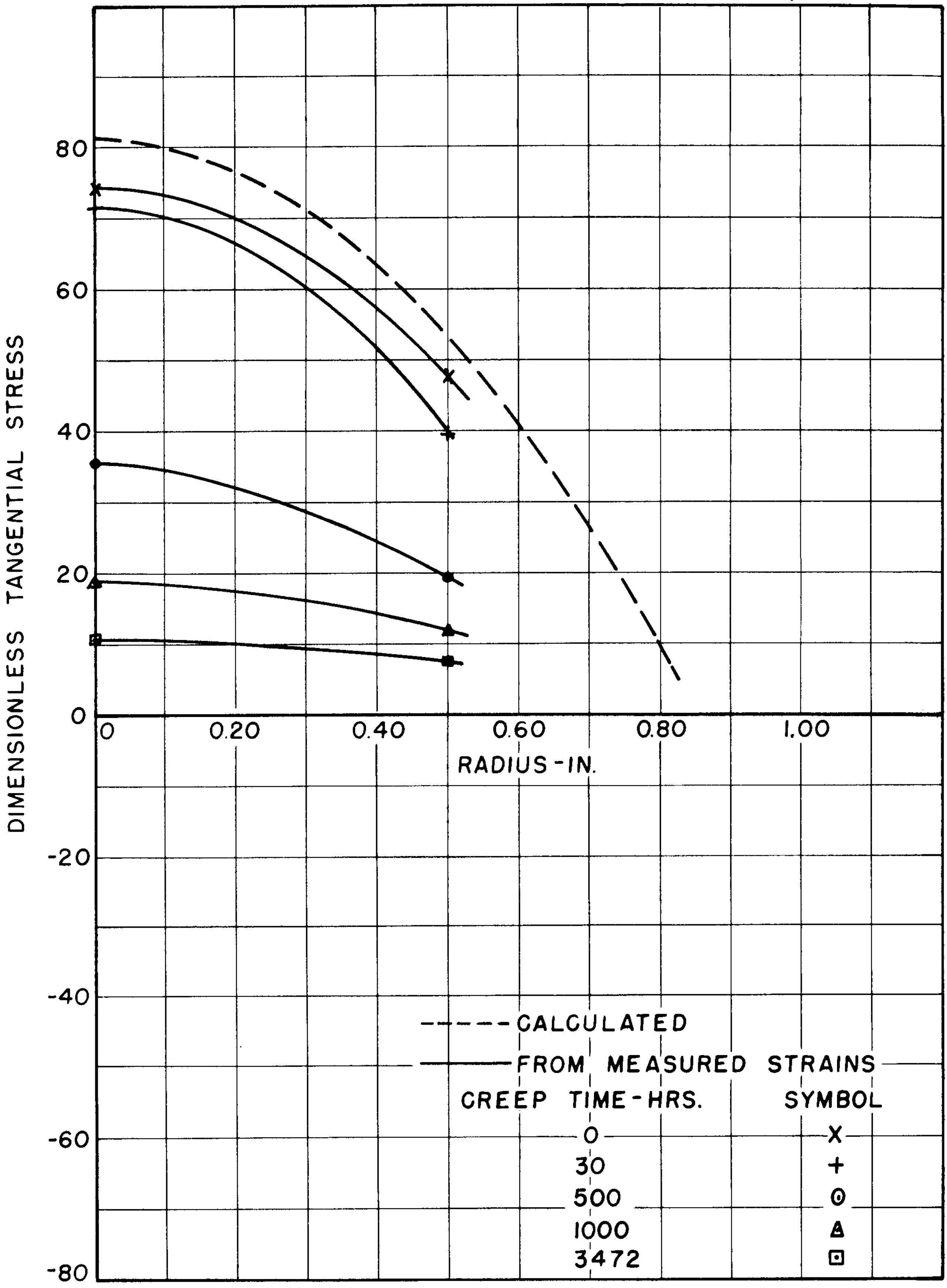

FIGURE 8. TOTAL TANGENTIAL STRESS AT OUTSIDE SURFACE OF HEAD VS. RADIUS

UNCLASSIFIED
ORNL-LR-DWG. 30490

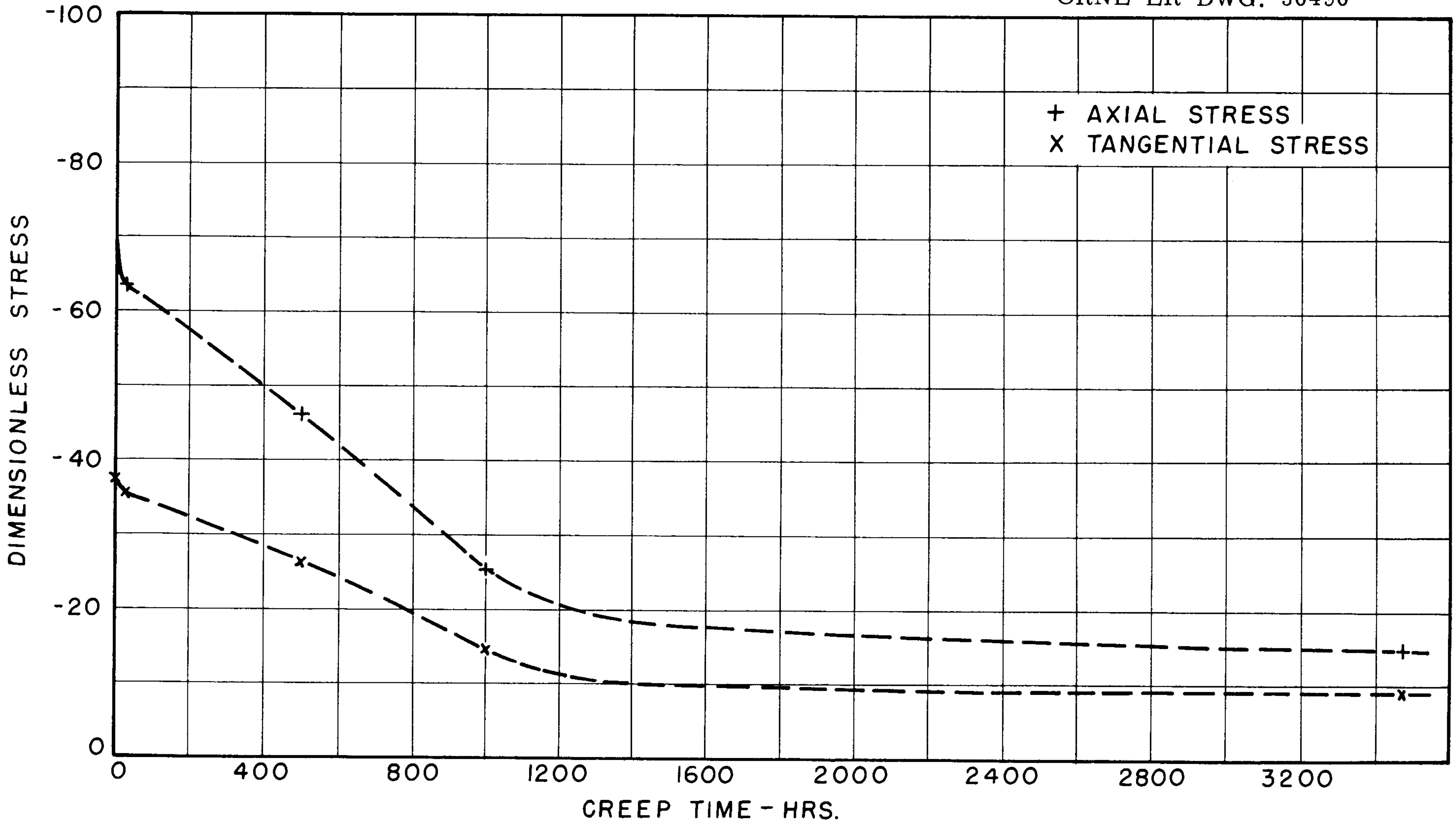

FIGURE 9. TOTAL STRESS AT OUTSIDE SURFACE OF CYLINDER VS. CREEP TIME-STATION 1

UNCLASSIFIED
ORNL-LR-DWG. 30491

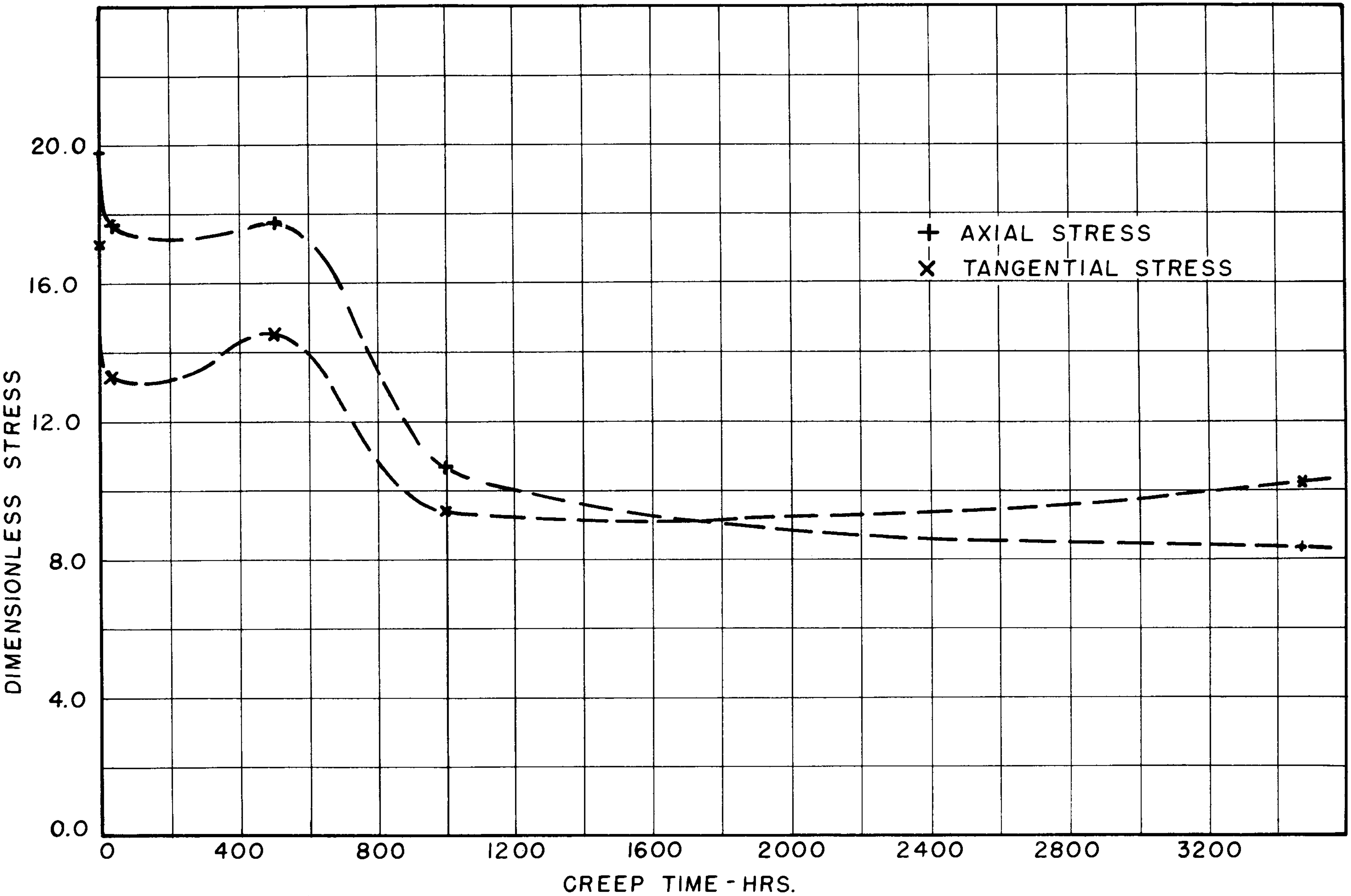

FIGURE 10. TOTAL STRESSES AT OUTSIDE SURFACE OF CYLINDER VS. CREEP TIME-STATION 3

UNCLASSIFIED
ORNL-LR-DWG. 30492

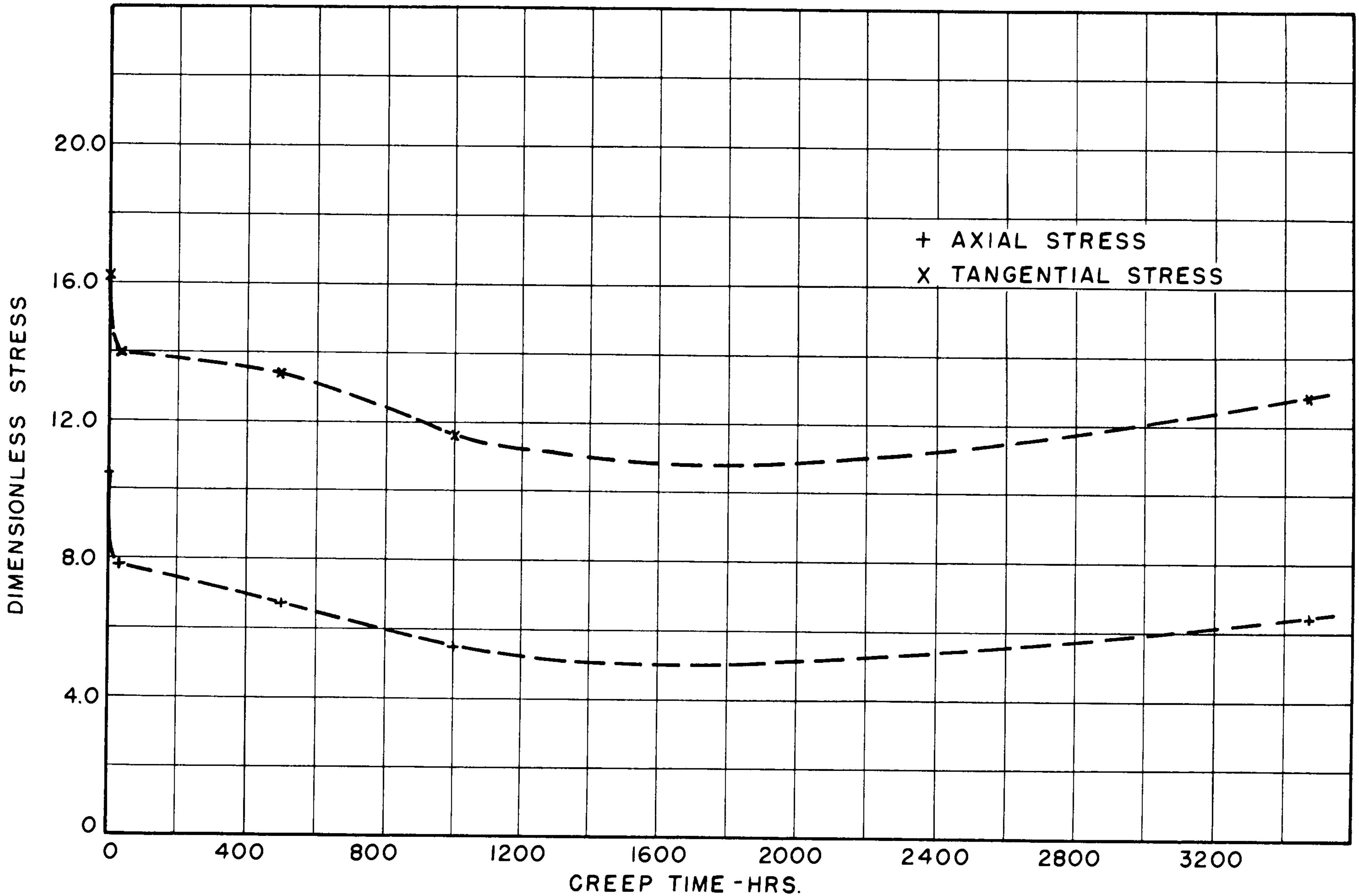

FIGURE 11. TOTAL STRESSES AT OUTSIDE SURFACE OF CYLINDER VS. CREEP TIME — STATION 5

UNCLASSIFIED
ORNL-LR-DWG. 30493

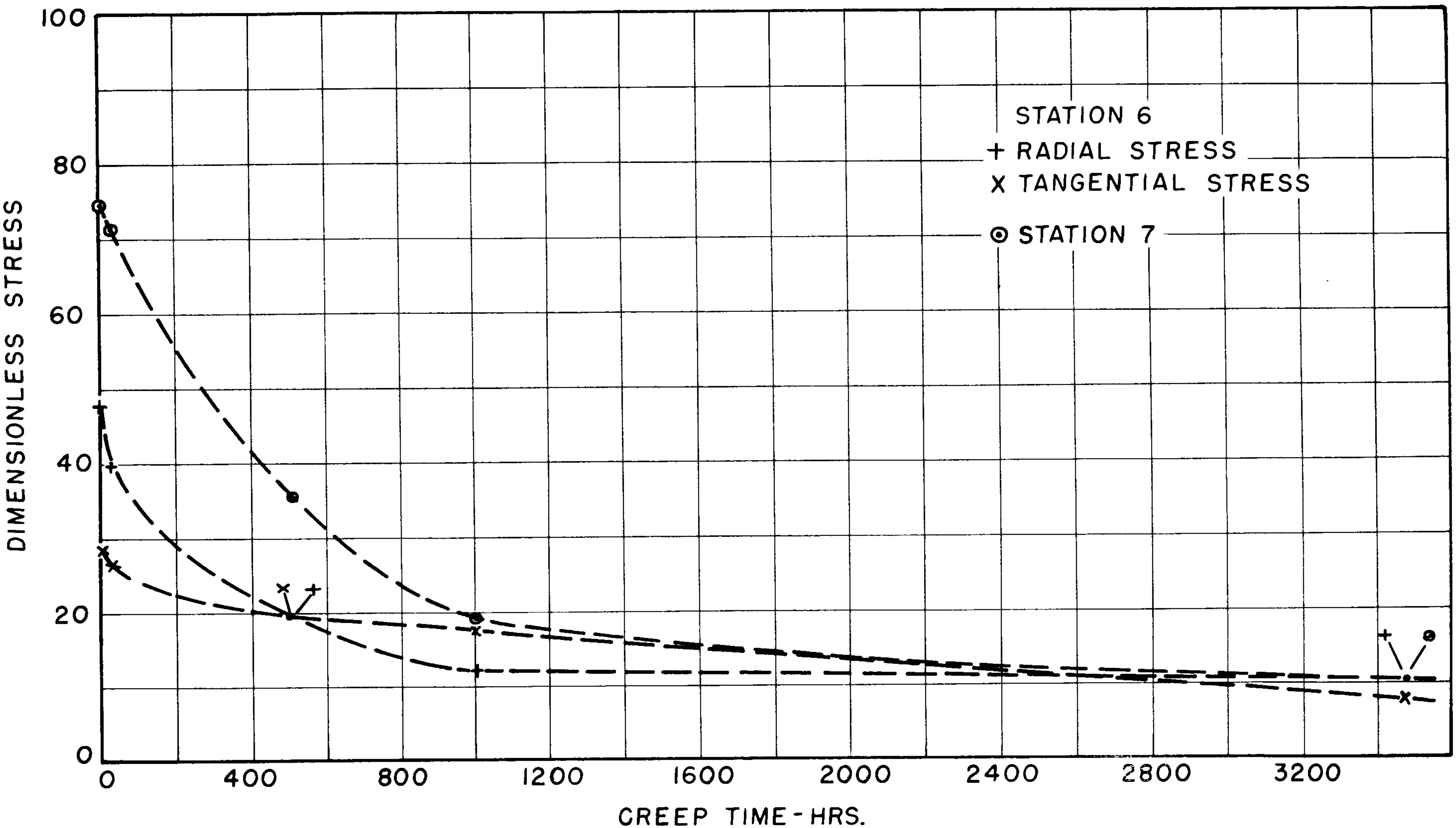

FIGURE 12. TOTAL STRESSES AT OUTSIDE SURFACE OF HEAD VS. CREEP TIME

UNCLASSIFIED
ORNL-LR-DWG. 30494

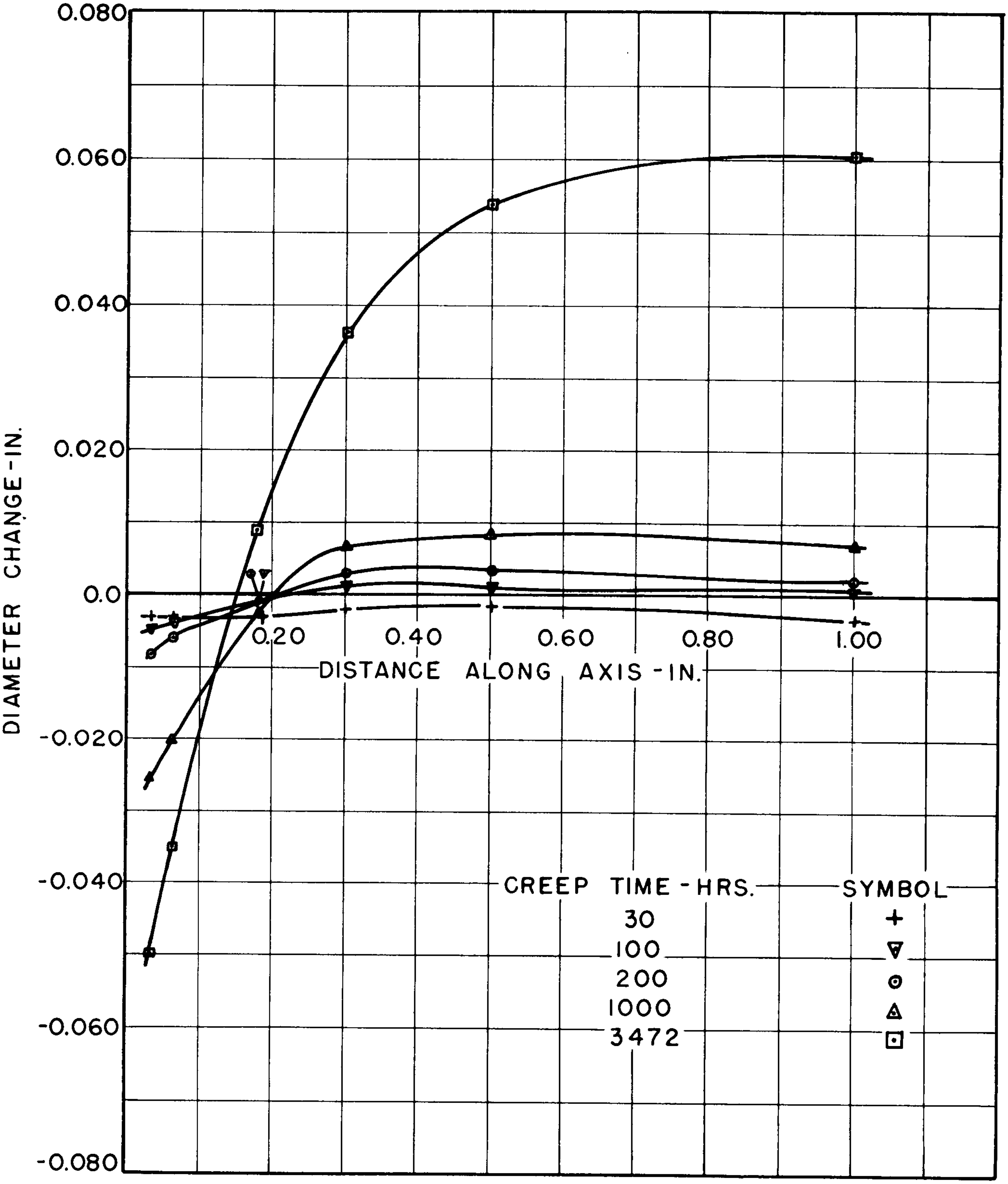

FIGURE 13. CHANGE IN OUTSIDE DIAMETER OF CYLINDER VS. DISTANCE ALONG AXIS

UNCLASSIFIED
ORNL-LR-DWG. 30495

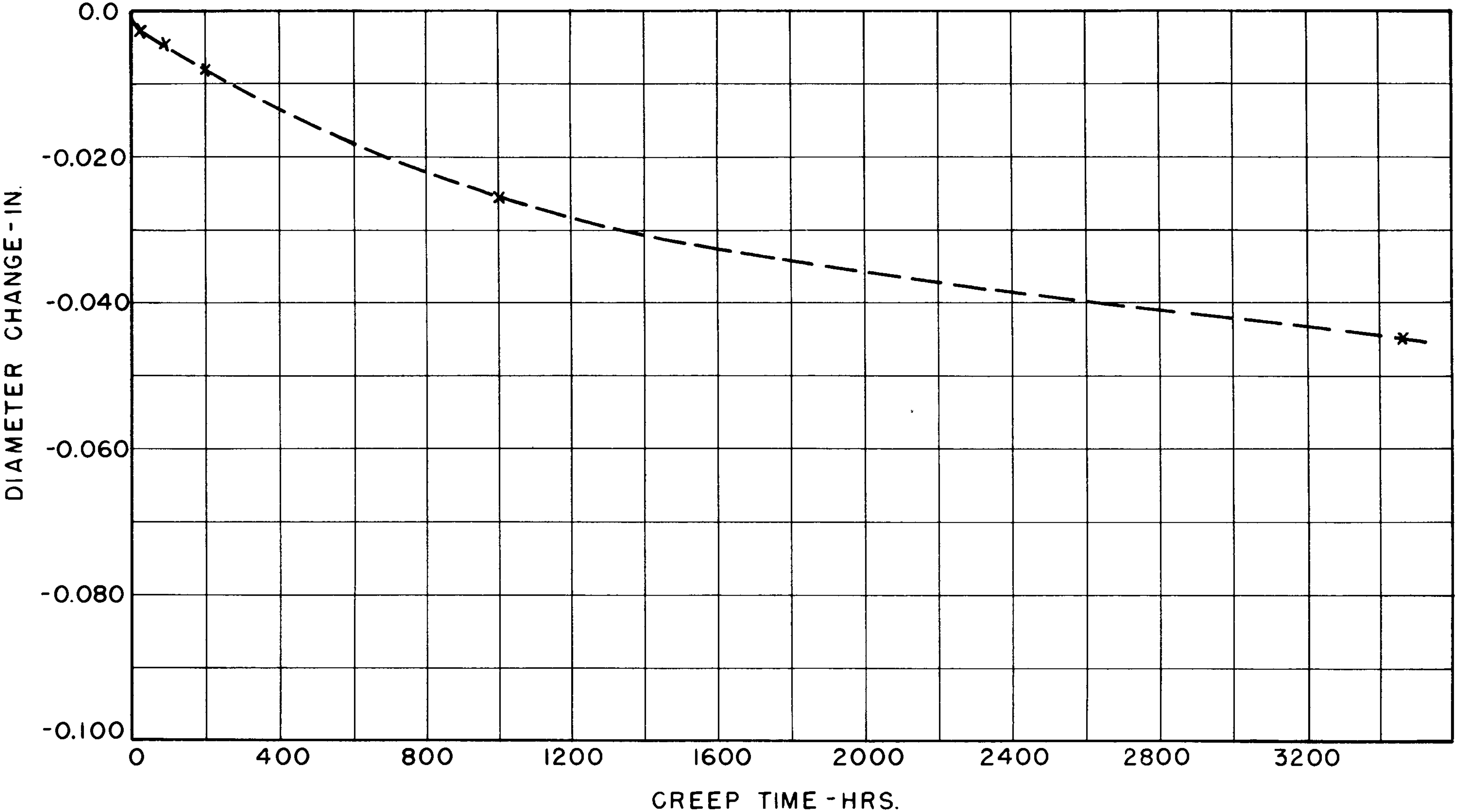

FIGURE 14. CHANGE IN OUTSIDE DIAMETER OF CYLINDER VS. CREEP TIME—STATION 1

UNCLASSIFIED
ORNL-LR-DWG. 30496

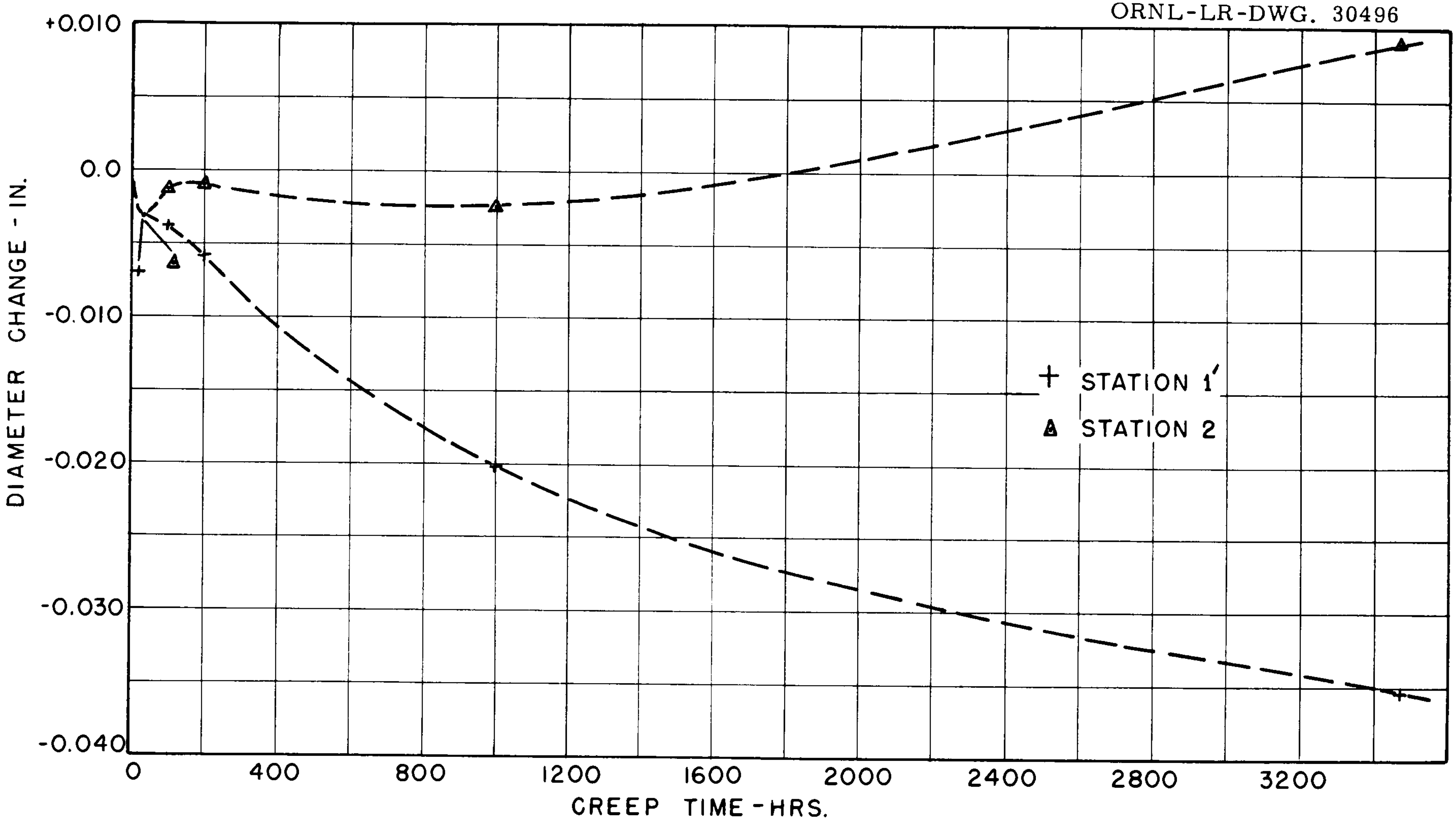

FIGURE 15. CHANGE IN OUTSIDE DIAMETER OF CYLINDER VS. CREEP TIME - STATIONS 1' & 2

UNCLASSIFIED
ORNL-LR-DWG. 30497

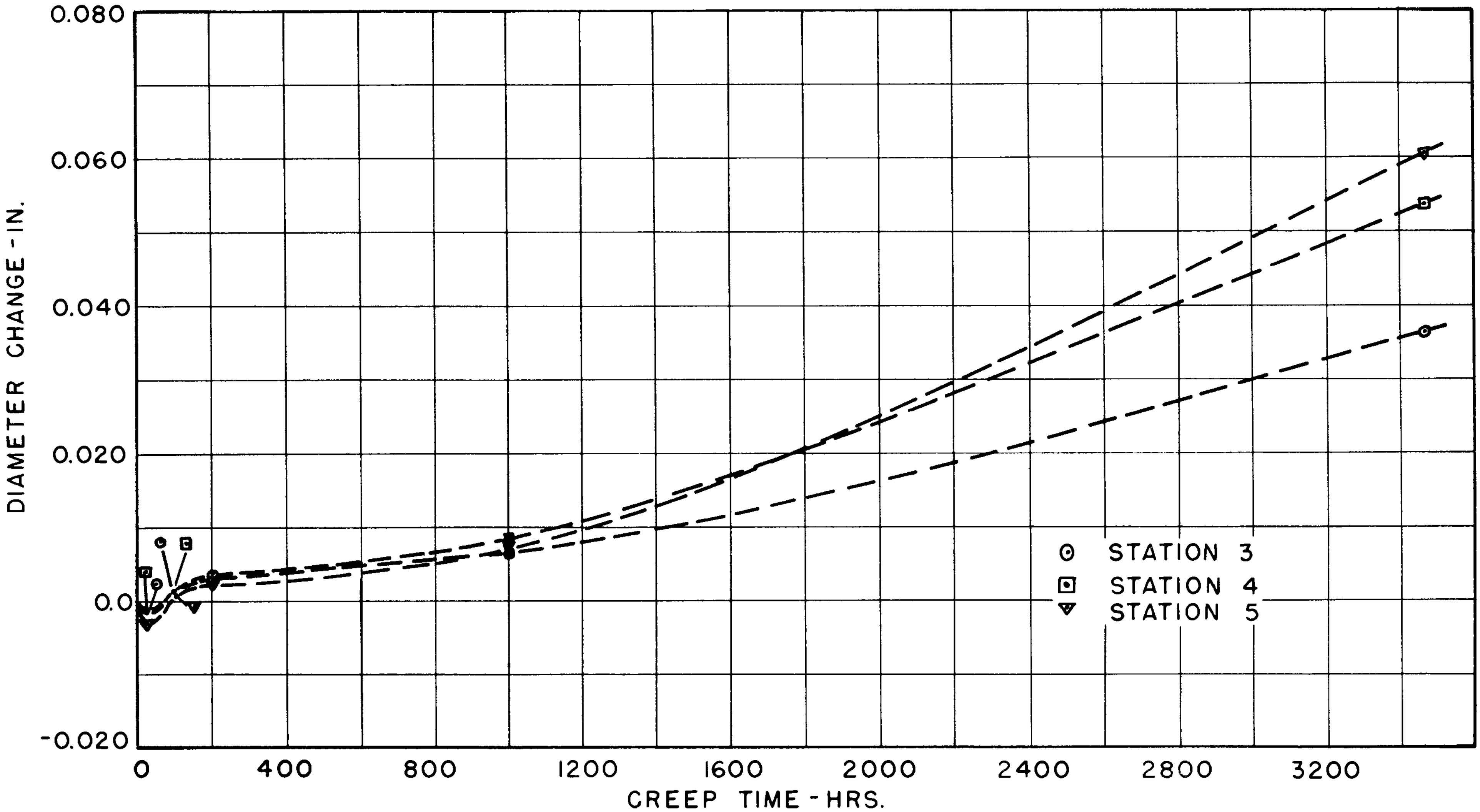

FIGURE 16. CHANGE IN OUTSIDE DIAMETER OF CYLINDER VS. CREEP TIME—STATIONS 3,4&5

UNCLASSIFIED
ORNL-LR-DWG. 30498

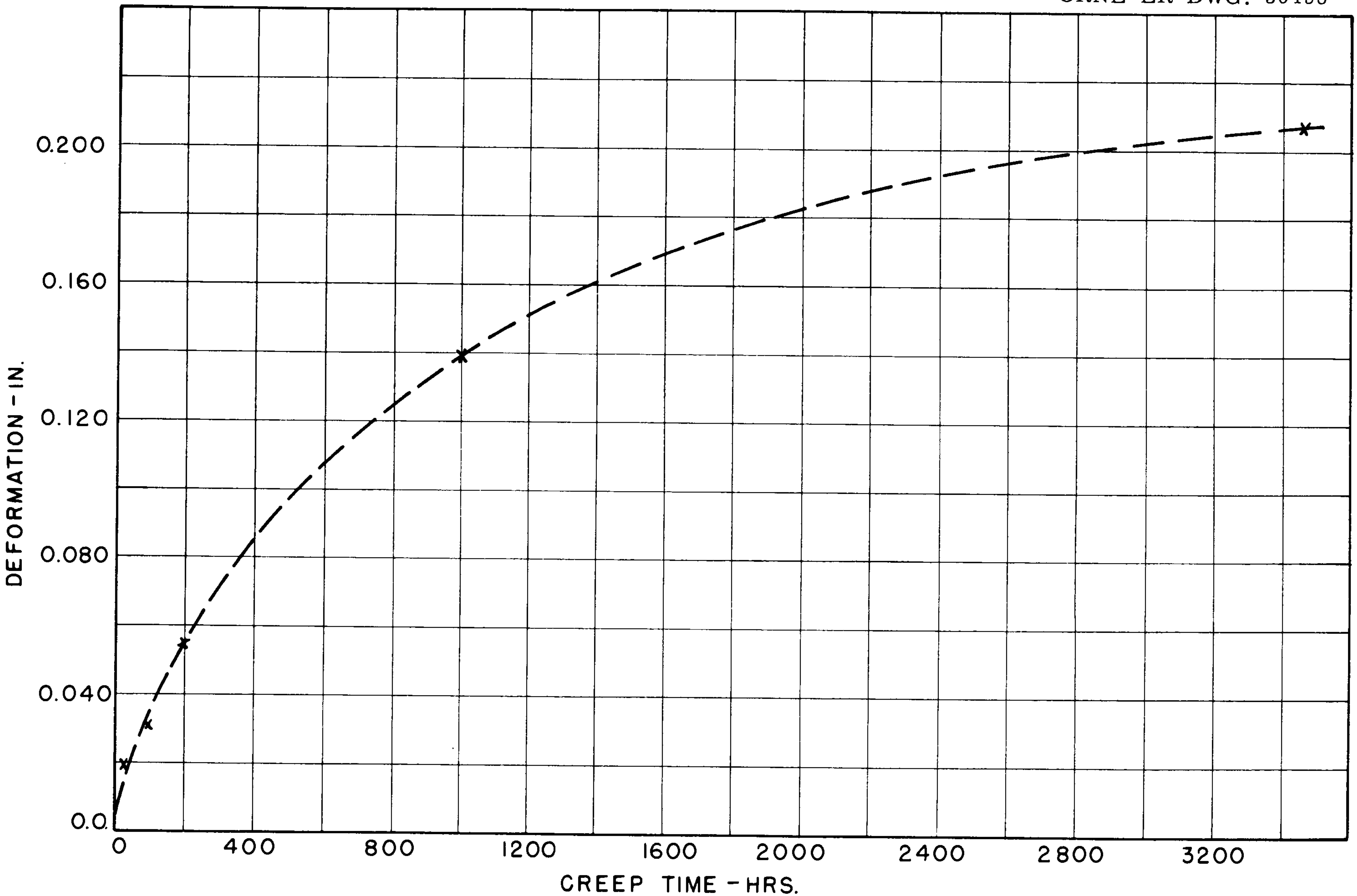

FIGURE 17. DEFORMATION AT CENTER OF HEAD VS. CREEP TIME

UNCLASSIFIED
Y-24414

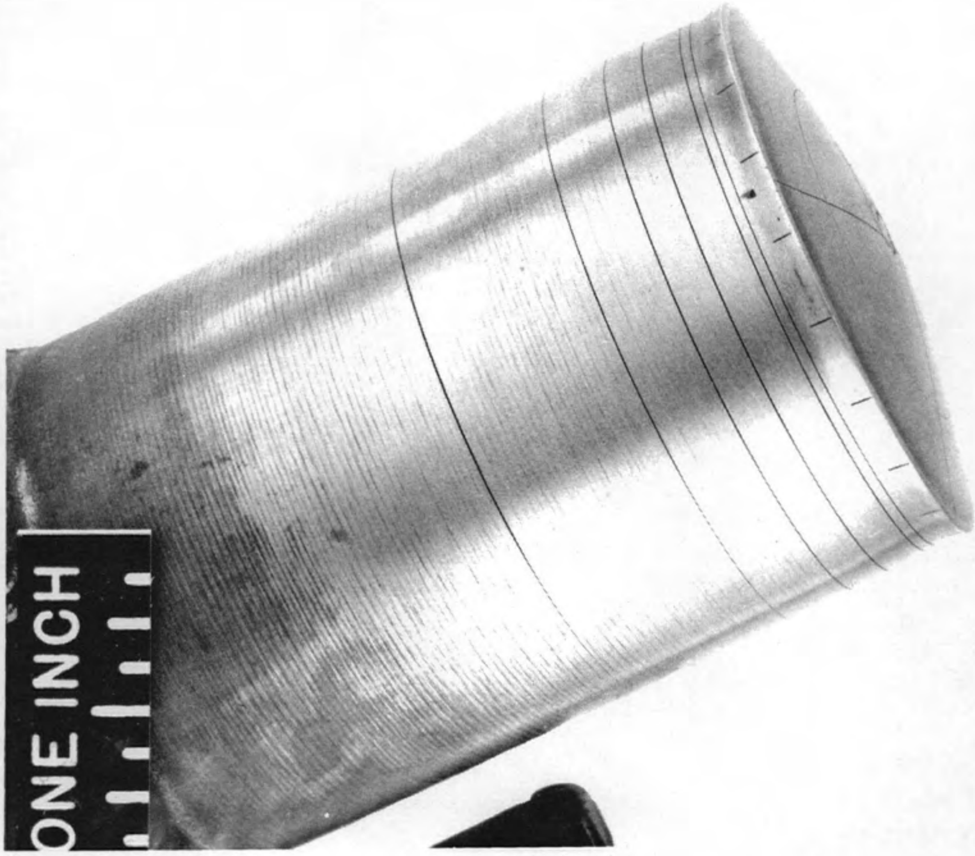

FIGURE 18. PRESSURE VESSEL AT END OF 1000 HRS. OF CREEP

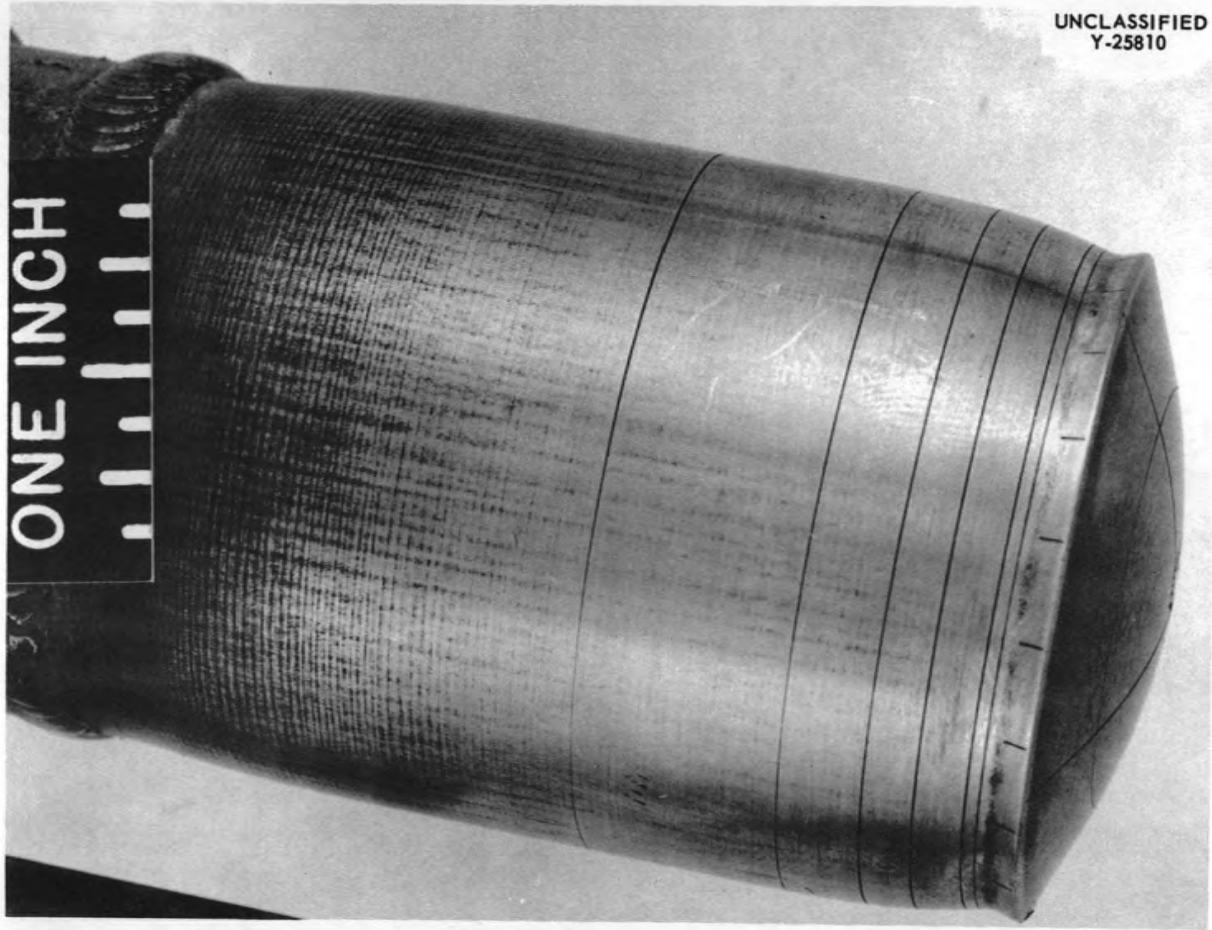

FIGURE 19. PRESSURE VESSEL AT END OF 3472 HRS. OF CREEP

UNCLASSIFIED
PHOTO 31243

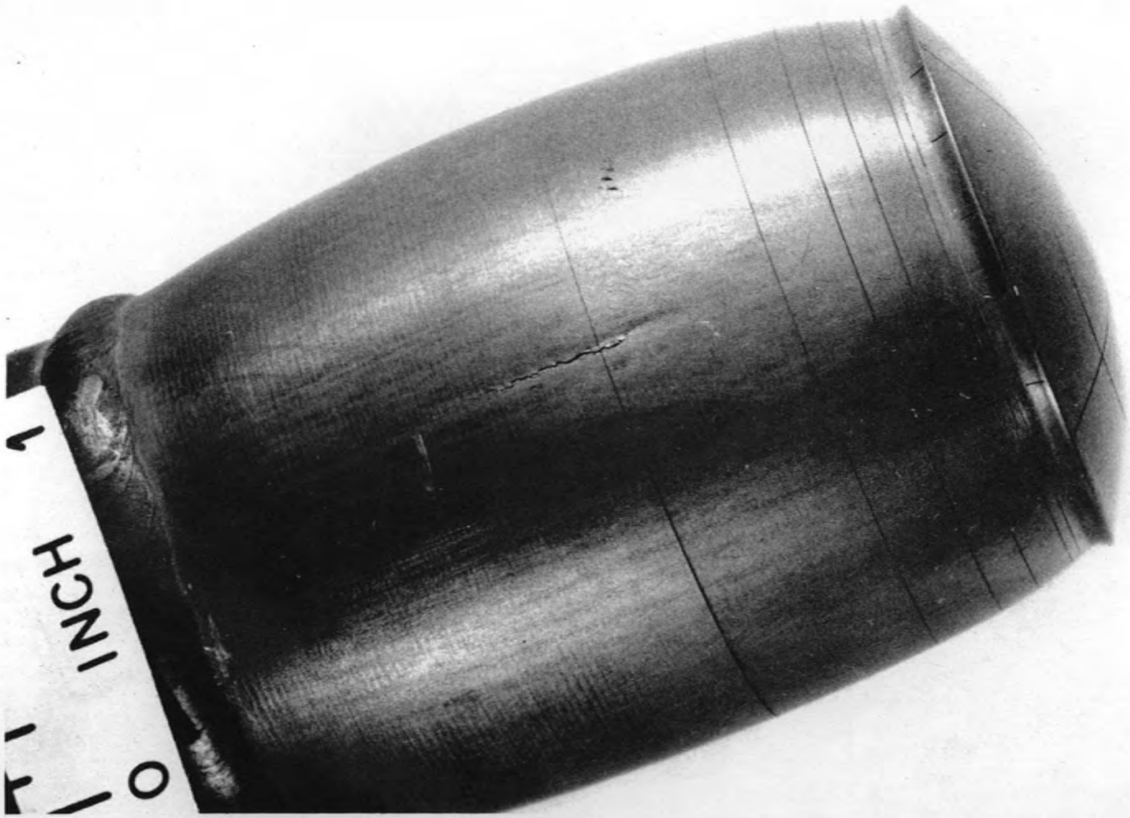

FIGURE 20. PHOTOGRAPH OF VESSEL SHOWING REGION OF FAILURE

BIBLIOGRAPHY

(1) Formulas for Stress and Strain, R. J. Roark, McGraw-Hill Book Company, Inc., New York, Third Edition, 1954, p. 277.

(2) Theory of Plates and Shells, S. Timoshenko, McGraw-Hill Book Company, Inc., New York, 1940.

(3) Strength of Materials, Part II, S. Timoshenko, D. Van Nostrand Company, Inc., New York, Second Edition, 1941.

(4) "Analysis of Stresses in Circular Plates and Rings", E. O. Holmberg and Karl Axelson, Transactions A.S.M.E., Vol. 54, 1932, APM 54-2, pp. 13-28.

(5) Strength of Materials, Part I, S. Timoshenko, D. Van Nostrand Company, Inc., New York, Third Edition, 1955, pp. 54-55.

ORNL-2537
Reactors-General
TID-4500 (13th ed., Rev.)

INTERNAL DISTRIBUTION

1. C. E. Center
2. Biology Library
3. Health Physics Library
4-5. Central Research Library
6. Reactor Experimental Engineering Library
7-26. Laboratory Records Department
27. Laboratory Records, ORNL R.C.
28. D. S. Billington
29. F. F. Blankenship
30. E. P. Blizard
31. A. L. Boch
32. C. J. Borkowski
33. G. E. Boyd
34. E. J. Breeding
35. R. B. Briggs
36. D. W. Cardwell
37. R. A. Charpie
38. F. L. Culler
39. L. B. Emlet (K-25)
40. D. E. Ferguson
41. A. P. Fraas
42. J. H. Frye, Jr.
43. W. R. Grimes
44. E. Guth
45. C. S. Harrill
46. H. W. Hoffman
47. A. Hollaender
48. A. S. Householder
49. W. H. Jordan
50. G. W. Keilholtz
51. M. T. Kelley
52. J. A. Lane
53. R. S. Livingston
54. H. G. MacPherson
55. W. D. Manly
56. J. R. McNally
57. K. Z. Morgan
58. J. P. Murray (Y-12)
59. M. L. Nelson
60. A. M. Perry
61. H. W. Savage
62. A. W. Savolainen
63. E. D. Shipley
64. M. J. Skinner
65. A. H. Snell
66. J. A. Swartout
67. E. H. Taylor
68. A. M. Weinberg
69. C. E. Winters
70. M. Bender
71. R. D. Cheverton
72. B. Y. Cotton
73. D. A. Douglas
74. L. P. Epel
75. J. Foster
76. W. T. Furgerson
77. R. S. Holcomb
78-97. B. L. Greenstreet
98. R. W. Holland
99. P. R. Kasten
100. J. L. Kerrebrock
101. B. Kinyon
102. M. E. Lackey
103-106. R. L. Maxwell
107. J. J. Meador
108. R. V. Meghreblian
109. R. D. Schultheiss
110. R. W. Swindeman
111. W. L. Scott
112. F. J. Stanek
113. G. Samuels
114. J. R. Tallackson
115. E. R. Volk
116. G. D. Whitman
117. F. J. Witt
118. J. W. Woods
119. M. M. Yarosh
120. ORNL - Y-12 Technical Library, Document Reference Section

EXTERNAL DISTRIBUTION

121. Pratt and Whitney Aircraft (1 copy each to C. C. Bigelow, C. R. Kennedy, C. H. Wells, and S. E. Moore)
122. R. M. Evan-Iwanowski, Syracuse University
123. F. A. Field, Lockheed Aircraft
124-709. Given distribution as shown in TID-4500 (13th ed., Rev.) under Reactors-General category (75 copies - OTS)